GJB2 mutation p.Asp50Asn and may contribute the proband's phenotype. Nevertheless, the limited scope of this study (single case report) does not allow us to determine the clinical significance of p.Ser59Arg in K17, and the influence of other genetic and epigenetic factors cannot be excluded.

*Department of Dermatology, Hokkaido University Graduate School of Medicine, North 15 West 7, Sapporo 060-8638, Japan
†Department of Dermatology, University of Miyazaki Faculty of Medicine, Miyazaki, Japan
‡Department of Dermatology, Nagoya University Graduate School of Medicine, Nagoya, Japan
E-mail: natsuga@med.hokudai.ac.jp

K. NATSUGA*
S. SHINKUMA*
M. KANDA*
Y. SUZUKI*
N. CHOSA†
Y. NARITA†
M. SETOYAMA†
W. NISHIE*
M. AKIYAMA*‡
H. SHIMIZU*

References

1 Mazereeuw-Hautier J, Bitoun E, Chevrant-Breton J *et al.* Keratitis–ichthyosis–deafness syndrome: disease expression and spectrum of connexin 26 (GJB2) mutations in 14 patients. Br J Dermatol 2007; **156**:1015–19.
2 Jan AY, Amin S, Ratajczak P *et al.* Genetic heterogeneity of KID syndrome: identification of a Cx30 gene (GJB6) mutation in a patient with KID syndrome and congenital atrichia. J Invest Dermatol 2004; **122**:1108–13.
3 Richard G, White TW, Smith LE *et al.* Functional defects of Cx26 resulting from a heterozygous missense mutation in a family with dominant deaf-mutism and palmoplantar keratoderma. Hum Genet 1998; **103**:393–9.
4 del Castillo I, Villamar M, Moreno-Pelayo MA *et al.* A deletion involving the connexin 30 gene in nonsyndromic hearing impairment. N Engl J Med 2002; **346**:243–9.
5 Kanda M, Natsuga K, Nishie W *et al.* Morphological and genetic analysis of steatocystoma multiplex in an Asian family with pachyonychia congenita type 2 harbouring a KRT17 missense mutation. Br J Dermatol 2009; **160**:465–8.
6 Nadeau JH. Modifier genes in mice and humans. Nat Rev Genet 2001; **2**:165–74.
7 Szeverenyi I, Cassidy AJ, Chung CW *et al.* The Human Intermediate Filament Database: comprehensive information on a gene family involved in many human diseases. Hum Mutat 2008; **29**:351–60.
8 Steinert PM, Mack JW, Korge BP *et al.* Glycine loops in proteins: their occurrence in certain intermediate filament chains, loricrins and single-stranded RNA binding proteins. Int J Biol Macromol 1991; **13**:130–9.
9 Terrinoni A, Puddu P, Didona B *et al.* A mutation in the V1 domain of K16 is responsible for unilateral palmoplantar verrucous nevus. J Invest Dermatol 2000; **114**:1136–40.
10 Adzhubei IA, Schmidt S, Peshkin L *et al.* A method and server for predicting damaging missense mutations. Nat Methods 2010; **7**:248–9.

Funding sources: none.

Conflicts of interest: none declared.

ASBMT
American Society for Blood and Marrow Transplantation

Decreased Serum Testosterone Levels in Long-Term Adult Survivors with Fatty Liver after Childhood Stem Cell Transplantation

Hiromi Hyodo,[1] Hiroyuki Ishiguro,[1] Yuichiro Tomita,[1] Hiromitsu Takakura,[1] Takashi Koike,[1] Takashi Shimizu,[1] Tsuyoshi Morimoto,[1] Hiromasa Yabe,[2] Miharu Yabe,[3] Sei-ichiro Kojima,[4] Koichi Shiraishi,[4] Takashi Minemura,[5] Shunichi Kato[2]

Fatty liver and male gonadal dysfunction are potential late effects of therapy in adult survivors treated with stem cell transplantation (SCT) in childhood. Obesity and metabolic syndrome also are associated with low serum testosterone levels in the general population. However, the relationship between the degree of fatty liver and changes in serum testosterone levels in adult survivors has not been fully studied. We reviewed the clinical records of 34 male patients who received allogeneic SCT in childhood or adolescence. The median age at SCT was 10.0 years, and the median follow-up after SCT was 15.9 years. All but one patient showed no tendency toward overweight/obesity during the follow-up period. Fatty liver was diagnosed by ultrasound in 15 patients at 4 to 20 years after SCT. Patients who received cranial radiation therapy before SCT were more likely to develop fatty liver and insulin resistance. Moreover, fatty liver was statistically associated with decreased serum testosterone levels, whereas nonfatty liver was not (median, 527 ng/dL [range, 168-944 ng/dL] versus 302 ng/dL [165-698 ng/dL]; $P < .0001$). Changes in testosterone levels after SCT are affected not only by primary gonadal dysfunction but also by subsequent development or exacerbation of fatty liver.

Biol Blood Marrow Transplant ■: 1-9 (2012) © 2012 American Society for Blood and Marrow Transplantation

KEY WORDS: Insulin resistance, Gonadal function, Cranial radiation therapy, Childhood cancer survivor, Obesity

INTRODUCTION

Continuing advances in the management of childhood malignancies are producing a rapidly enlarging group of childhood cancer survivors [1-3]. With survival rates currently at 70% to 80%, an estimated one in 700 of the young adult population in Japan is a long-term survivor of childhood cancer [4,5]. Children and adult survivors commonly experience morbidity, generally related to the treatment they received to cure their cancer rather than to the cancer itself. Treatment-related morbidity is extraordinarily diverse. Childhood cancer survivors are at significant risk for developing late effects after successful cancer treatment during childhood. In particular, endocrine system disorders are common, affecting up to 40% of childhood cancer survivors and include gonadal dysfunction, metabolic disorders, thyroid dysfunction, and growth impairment [6-11].

Fatty liver is associated with metabolic abnormalities characterized by obesity [12], type 2 diabetes mellitus (DM) [13], dyslipidemia [14], and hypertension [15], each of which also carries a cardiovascular disease risk. Moreover, fatty liver is increasingly recognized as a major cause of liver-related morbidity and mortality in the general population because of its potential to progress to cirrhosis and liver failure [16]. Numerous epidemiologic investigations in the general population have established associations between low serum testosterone level and obesity and metabolic syndrome [17-19]; however, the mechanism underlying these conditions is incompletely understood. In particular, whether low serum testosterone causes metabolic syndrome or vice versa has not been clarified. We hypothesized that fatty liver with insulin resistance may be considered as the cause of reduced testosterone levels in adult childhood cancer survivors.

From the [1]Department of Pediatrics; [2]Department of Cell Transplantation and Regenerative Medicine; [3]Department of Laboratory Medicine; [4]Division of Gastroenterology, Department of Internal Medicine; and [5]Department of Clinical Laboratory, Tokai University School of Medicine, Kanagawa, Japan.

Financial disclosure: See Acknowledgments on page 8.

Correspondence and reprint requests: Hiroyuki Ishiguro, MD, Department of Pediatrics, Tokai University School of Medicine, 143 Shimokasuya, Isehara, Kanagawa 259-1193, Japan (e-mail: h-ishi@is.icc.u-tokai.ac.jp).

Received December 26, 2011; accepted January 9, 2012

1083-8791/$36.00
doi:10.1016/j.bbmt.2012.01.004

Although metabolic syndrome and gonadal dysfunction in adult survivors have been well documented, a longitudinal study investigating the relationship between the degree of fatty liver and changes in gonadal function in survivors of childhood stem cell transplantation (SCT) has not yet been reported, and the mechanism of these conditions has not been completely elucidated. To test our hypothesis, we performed a longitudinal retrospective study of adult male survivors of childhood cancer treated with SCT to investigate the relationship between fatty liver and gonadal function.

METHODS

Patients

We reviewed the clinical records of 98 male patients who underwent SCT at Tokai University Hospital between 1982 and 1997 and had annual follow-up. Inclusion criteria were survival for at least 5 years after SCT, age at least 18 years at the last evaluation, and no past history of or laboratory findings suggesting liver dysfunction or endocrine or metabolic abnormalities before SCT. Thirty-four adult survivors met these criteria and were included in this analysis. In these 34 patients, the median age at the time of SCT was 10.0 years, the median age at the last evaluation was 25.1 years, and the median duration of follow-up after SCT was 16.3 years (Table 1). To examine the risk factors for developing fatty liver, the study population was categorized into four groups according to age at SCT, primary disease, presence of fatty liver, doses of radiation to the brain and testes, and conditioning regimen received: the cranial radiation therapy (CRT) plus total body irradiation (TBI) group, the TBI group, the thoracoabdominal irradiation (TAI) group, and the chemotherapy (Chemo) group. Patient characteristics are summarized in Table 1. Written informed consent was obtained from all patients and/or their parents. This study was approved by Tokai University's Clinical Research Review Committee.

Transplantation Procedure

In addition to conventional chemotherapy, three patients with acute lymphoblastic leukemia (ALL) and one patient with non-Hodgkin lymphoma (NHL) received prophylactic CRT (one with 12 Gy and three with 18 Gy) at 1 to 5 years before SCT. In 28 patients, conditioning regimens consisted of irradiation with or without cyclophosphamide (CY) and/or other drugs; 8 to 12 Gy of TBI was given in four to six fractions for patients with malignant diseases, and 6 to 8 Gy of TAI was given in three or four fractions for patients with nonmalignant diseases. The testes were shielded from radiation during the TAI procedures. The remaining six patients received conditioning without irradiation. Prophylaxis against graft-versus-host disease (GVHD) varied during the time period, with methotrexate, cyclosporine, or a combination of the two drugs used.

Anthropometric Measures of Body Composition

All patients had achieved their final height at the last evaluation. Body mass index (BMI) was calculated as weight in kilograms divided by the height in meters squared (kg/m^2). Patients with a BMI $\geq$25 kg/m^2 were classified as overweight/obese, and those with a BMI $\leq$18.5 kg/m^2 were classified as underweight in accordance with World Health Organization criteria [20]. Waist circumference (WC) was measured at the level of the superior iliac crest. Abdominal adiposity was defined as a WC-to-height ratio >0.5 [21-23]. Bioelectronic impedance analysis was performed to measure body fat by (InnerScan; Tanita, Tokyo, Japan).

Evaluation of Fatty Liver

Fatty liver was evaluated by a total of 303 longitudinal ultrasound examinations performed in the 34 patients during the follow-up period. Up to 1994, Hitachi EUB340 (Hitachi, Tokyo, Japan) and Yokogawa RT2800 and RT3000 (GE Yokogawa Medical Systems, Tokyo, Japan) ultrasound systems were used to evaluate fatty liver. After 1995, this evaluation was done using an Aloka SSD 650CL system (Aloka, Tokyo, Japan). Of the four criteria used for the diagnosis of fatty liver—hepatorenal echo contrast (HRE), liver brightness (LB), deep attenuation (DA), and vascular blurring (VB)—the first two were used as definitive criteria, and the last two were taken into account as needed [24]. The degree of fatty liver was classified as follows: severe, both HRE and LB positive; moderate, either HRE or LB positive and/or either DA or VB positive; or mild, HRE, LB, DA, and VB negative. In all cases, two gastroenterology specialists separately confirmed the diagnosis without access to detailed information about the patient's background. Abdominal computed tomography was performed in 23 patients, and the results were coordinated with fatty liver diagnosed by ultrasound, as described in detail elsewhere [9].

Evaluation of Glucose and Lipid Metabolism Profiles

An overnight fasting blood sample was obtained from all patients for the measurement of plasma glucose, plasma insulin, serum triglycerides (TG), serum total cholesterol (TC), serum high-density lipoprotein cholesterol (HDL-C), serum low-density lipoprotein-cholesterol (LDL-C), and serum-free fatty acid. To convert our data to SI units, multiply plasma glucose by 0.0555 (result in mmol/L), plasma insulin by

Table 1. Patient Characteristics

	All (n = 34)	Fatty Liver (n = 15)	Non-Fatty Liver (n = 19)	*P* Value[a]
Age at SCT, years, median (range)	10.0 (0.7-15.8)	8.8 (0.7-15.5)	10.5 (0.9-15.8)	.627
Age at last evaluation, years, median (range)	25.1 (18.0-36.0)	24.8 (18.0-36.0)	25.3 (18.0-33.2)	.945
Dollow-up duration after SCT, years, median (range)	16.3 (6.7-27.7)	16.0 (6.7-27.7)	16.8 (7.6-24.8)	1
Primary disease, n				
Malignant disease				
Acute lymphoblastic leukemia	8	5	3	
Acute myelogenous leukemia	6	3	3	
Chronic myelogenous leukemia	3	2	1	
Non-Hodgkin lymphoma	4	1	3	
Nonmalignant disease				
Aplastic anemia	8	2	6	
Other	5	2	3	
Cranial radiation before SCT, n	4	3	1	
Conditioning regimen for SCT, n				
TBI + cyclophosphamide + other drugs	20	9	11	
Thoracoabdominal irradiation + cyclophosphamide + other drugs	8	3	5	
Chemotherapy	6	3	3	
Radiation therapy, n				
Brain 0 Gy	14	6	8	
Brain ≥8 Gy	20	9	11	
Testes 0 Gy	14	6	8	
Testes 8-12 Gy	20	9	11	

[a]For comparison of fatty liver and non-fatty liver.

6.945 (pmol/L), serum TG by 0.0113 (mmol/L), and serum TC, serum HDL-C, and serum LDL-C by 0.0259 (mmol/L).

Insulin resistance was estimated by the homeostatic model assessment of insulin resistance (HOMA-IR) using the formula fasting plasma insulin (mU/L) × plasma glucose (mg/dL)/405, with a value ≥2.5 indicating insulin resistance. The oral glucose tolerance test (OGTT) was performed in 25 patients for evaluation of glucose and insulin metabolism. For the OGTT, the patient was given glucose at 1.75 g/kg (maximum, 75 g) after a 12-h overnight fast, and samples for measurement of plasma glucose and plasma insulin were drawn at baseline and every 30 minutes for up to 120 minutes. Hyperinsulinemia was defined as a fasting plasma insulin value of ≥13 mU/L or a peak plasma insulin level ≥150 mU/L on the OGTT. Definitions of DM and impaired glucose tolerance were based on Japan Diabetes Society criteria. The presence of either type 1 or type 2 DM was diagnosed by a fasting plasma glucose level ≥126 mg/dL and/or a plasma glucose level ≥200 mg/dL at 2 h after the glucose load. A random plasma glucose value >200 mg/dL was also considered to indicate DM. A fasting plasma glucose level <110 mg/dL and a 2-h plasma glucose level <140 mg/dL were considered normal values. Impaired glucose tolerance was diagnosed in patients with values that were not normal but that did not indicate DM.

Evaluation of Metabolic Syndrome

Metabolic syndrome was defined according to the criteria published by a committee convened to establish the definition and diagnostic criteria of metabolic syndrome in Japan [25]: central obesity (WC ≥85 cm in males) and the presence of at least two of the following factors—serum TG ≥150 mg/dL and/or HDL-C <40 mg/dL, systolic blood pressure ≥130 mm Hg and/or diastolic blood pressure ≥85 mm Hg, and fasting plasma glucose ≥110 mg/dL.

Evaluation of Endocrine Function

Onset of puberty was defined as a testicular volume ≥4 mL [26]. Testicular volume was measured with an orchidometer, as described by Prader [27]. Testicular Leydig cell function and germinal epithelium damage were evaluated by measurement of basal serum luteinizing hormone (LH) level, basal serum follicle-stimulating hormone (FSH) level, and serum testosterone level before SCT and annually during the follow-up period. The normal basal serum LH and FSH levels at our institutions were <9 mIU/mL and <14 mIU/mL, respectively, and the normal range of serum testosterone of the patients in their 20s and 30s was 131-871 ng/dL. Partial Leydig cell dysfunction and partial germinal epithelium damage were defined by either increased basal LH level (≥15 IU/mL) or increased basal FSH level (≥20 IU/mL) with a normal testosterone level. To convert to SI units, serum testosterone values were multiplied by 0.0347 (results in nmol/L). Plasma sex hormone-binding globulin (SHBG) levels and free testosterone measurements were performed by Special Reference Laboratories (Tachikawa, Japan). All analyses except plasma SHBG and free testosterone were performed in our hospital's routine clinical laboratory. Blood draws for endocrine tests were performed with the patient in a morning fasting state, to avoid diurnal hormonal variation.

Statistical Analysis

Because the data had a skewed distribution, values are presented as median and range. Differences in anthropometric and laboratory variables among groups were analyzed using the Kruskal-Wallis test with Dunn's multiple comparison test. The Mann-Whitney test was used to compare differences between groups. Kaplan-Meier survival curves were constructed to assess the probability of fatty liver, and the log-rank test was used to compare survival curves. All statistical analyses were performed with the statistical package GraphPad Prism 5 for Mac OS X (GraphPad Software, La Jolla, CA). A P value <.05 was considered statistically significant.

RESULTS

Anthropometrics

Among the 34 patients, only one (unique patient number [UPN] 105), who had received chemotherapy only, had a BMI >25 kg/m^2 (26.2 kg/m^2) at the last evaluation. However, 11 patients had a BMI <18.5 kg/m^2 (one patient in the CRT+TBI group, seven patients in the TBI group, two patients in the TAI group, and one patient in the Chemo group). No patient satisfied the criteria for metabolic syndrome, although three patients had a WC >85 cm (one with a WC of 86.7 cm in the CRT+TBI group, one with a WC of 90.0 cm in the TAI group, and one with a WC of 92.2 cm in the Chemo group).

Fatty Liver

All 34 patients exhibited liver function within the normal range during the follow-up period, although one patient who received TBI (UPN 118) showed a transient increase in transaminase levels after SCT, and two patients had a positive hepatitis C virus-RNA test result (UPNs 64 and 100 in the TAI group). Information on daily alcohol consumption was obtained from all patients by self-report. The majority of the patients were nondrinkers or drank only minimally. Fatty liver was diagnosed in 15 patients (44%) by ultrasound during the follow-up period (Figure 1). The patients with fatty liver showed no tendency toward overweight/obesity during the follow-up period, however; the mean BMI in these patients was 18.8 kg/m^2 (range, 15.9-23.0 kg/m^2) at the last evaluation (Table 1). No relationships between the development of fatty liver and age at SCT, primary disease, or GVHD were observed. Concerning the mode of irradiation, the prevalence of fatty liver was higher in the CRT+TBI group compared with the TBI, TAI, and Chemo groups (75%, 38%, 38%, and 50%, respectively), although the difference among groups was not significant because of the small number of patients in each group (P = .070; log-rank test) (Figure 1). In five patients (UPN 91 in the CRT+TBI group, UPNs 1 and 11 in the TBI group, UPN 215 in the TAI group, and UPN 255 in the Chemo group), fatty liver improved with exercise and dietary regimens provided by physicians and dieticians during the follow-up period (Figure 1).

Evaluation of Lipid and Glucose Metabolism

Studies of lipid and glucose metabolism were performed to investigate the mechanism of development of fatty liver in patients who underwent SCT. Median TG and HDL-C levels were statistically significantly different between patients with fatty liver and those without fatty liver (Table 2). Moreover, the presence of fatty liver was significantly associated with increased insulin resistance as determined by HOMA-IR score (P = .032).

Evaluation of Endocrine Function

Puberty started spontaneously in all patients according to increases in testicular volume (≥4 mL), and all patients had developed adult genitalia (Tanner stage V) at the last evaluation. Serum testosterone level reached the adult range at some point between adolescence and adulthood after SCT in all patients (data not shown). To clarify the relationship between testicular irradiation and serum testosterone levels, patients were divided into two groups, the testicular irradiation group and the no testicular irradiation group. The median serum testosterone level was not significantly different between the two groups (448 ng/dL in the testicular irradiation group versus 468 ng/dL in the no testicular irradiation group), but serum LH and FSH levels were significantly higher in the testicular irradiation group (9.6 mIU/mL and 33.0 mIU/mL versus 5.9 mIU/mL and 14.3 mIU/mL; P < .0001) (Figure 2A-C). These findings indicate that testicular irradiation did not affect testosterone production. On the other hand, the presence of fatty liver was statistically associated with decreased serum testosterone levels (median, 527 ng/dL [range, 168-944 ng/dL] in patients with fatty liver versus 302 ng/dL [165-698 ng/dL] in those without fatty liver; P < .0001). Moreover, severe fatty liver tended to be associated with lower median serum testosterone levels compared with moderate, mild, and nonfatty liver (273 ng/dL, 333 ng/dL, 345 ng/dL, and 530 ng/dL, respectively; P < .0001) (Figure 2D-F). Decreased serum testosterone levels were associated with the development and progression of fatty liver, and recovery of serum testosterone levels was observed after resolution of fatty liver by exercise and diet in three patients (UPNs 011, 044,

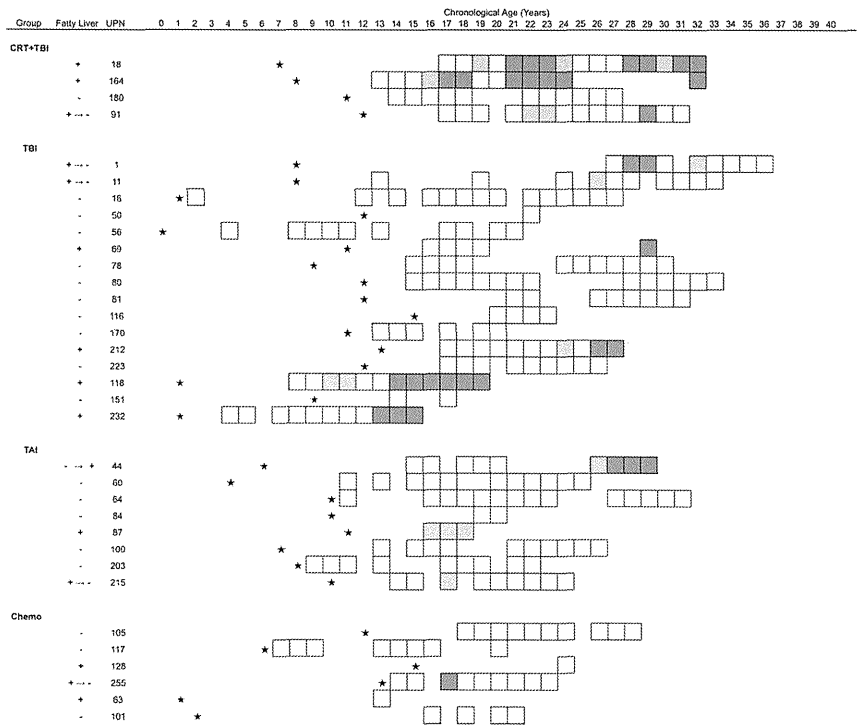

Figure 1. Changes in fatty liver in adult survivors of childhood SCT. The degree of fatty liver is classified as follows: □, absence; ▒, mild; ▒, moderate; ■, severe; +, existence; + → -, improved; ★, SCT.

and 212; Figure 3). Plasma SHBG levels were negatively correlated with HOMA-IR score (Spearman's rank correlation: r = -0.216; P = .375), but were positively correlated with serum testosterone levels (r = 0.498; P = .030).

DISCUSSION

This is the first study of adult survivors of childhood cancer treated with SCT to indicate a relationship between the degree of fatty liver and changes in serum testosterone levels after SCT. Our novel finding is that severe fatty liver presenting with insulin resistance is associated with decreased serum testosterone levels during the follow-up period after SCT. The incidence of fatty liver with decreased serum testosterone level was not associated with either overweight/obesity or metabolic syndrome in these patients who received SCT. These findings highlight the increased health risks in adult survivors of childhood SCT.

Fatty liver is increasingly recognized as a major cause of liver-related morbidity and mortality because of its potential to progress to cirrhosis and liver failure. In a previous study, we found an 18% to 27% prevalence of fatty liver in Japanese male subjects in their 20s and 30s [24]. However, in the current study, the prevalence of fatty liver was 44% in male adult survivors who were not overweight/obese during the follow-up period. These results indicate that SCT may affect the prevalence of fatty liver in adult survivors, and that these survivors are more likely to develop fatty liver compared with the general Japanese population. Moreover, the prevalence of fatty liver was greater in patients who received 24 to 30 Gy to the brain compared with those who received 8 to 12 Gy or 0 Gy. This suggests that radiation therapy to the brain may be a contributing factor to the development of fatty liver in adults who underwent SCT during childhood.

Table 2. Anthropometric Measurements, Liver Dysfunction Data, and Lipid and Glucose Metabolism Data in Adult Survivors of Childhood SCT

	All (n = 34)	Fatty Liver (n = 15)	Non-Fatty Liver (n = 19)	P Value[a]
Anthropometric measures				
Height, cm	159.1 (139.2-172.4)	158.5 (139.2-172.4)	159.7 (145.1-172.0)	.716
Weight, kg	47.5 (31.3-72.8)	46.1 (37.6-67.1)	49.2 (31.3-72.8)	.500
Waist circumference, cm	70.3 (53.0-92.2)	68.8 (61.5-82.0)	71.9 (53.0-92.2)	.728
BMI, kg/m^2	19.3 (13.8-26.2)	18.8 (15.9-23.0)	20.2 (13.8-26.2)	.659
WC-to-height ratio	0.4 (0.4-0.6)	0.5 (0.4-0.5)	0.4 (0.4-0.6)	.977
Body fat, %				
Liver dysfunction				
Aspartate aminotransferase, U/L	27 (15-74)	36 (20-74)	27 (15-68)	.183
Alanine aminotransferase, U/L	27 (13-183)	32 (15-183)	23 (13-99)	.167
Gamma-glutamyl transpeptidase, U/L	34 (14-224)	92 (14-224)	29 (19-175)	.042
Lipid and glucose metabolism				
TG, mg/dL	107 (35-409)	113 (67-409)	91 (35-185)	.038
TC, mg/dL	203 (148-294)	195 (157-294)	207 (148-250)	.851
HDL-C, mg/dL	63 (36-114)	47 (36-114)	67 (53-98)	.046
LDL-C, mg/dL	128 (71-892)	135 (86-892)	127 (71-676)	.805
Free fatty acid, mEq/L	0.60 (0.2-1.3)	0.60 (0.2-1.3)	0.50 (0.2-1.3)	.351
HOMA-IR	1.9 (0.5-9.4)	3.5 (0.9-9.4)	1.6 (0.5-6.3)	.032

Data are presented as median (range). To convert to SI units, multiply serum TG by 0.0113 (mmol/L) and multiply serum TC, serum HDL-C, and serum LDL-C by 0.0259 (mmol/L).
[a]For comparison of fatty liver and non-fatty liver.

The present study included an insufficient number of patients on which to base any definitive conclusions, however, and additional prospective and multicenter studies in larger populations are needed to investigate the mechanism of this effect.

Many previous studies have reported low plasma testosterone levels in men with metabolic syndrome or type 2 DM [28,29]. Visceral obesity suppresses testosterone production, and low plasma testosterone levels induce visceral obesity and insulin resistance. Kapoor et al [30] and others [31,32] reported randomized double-blind, placebo-controlled studies of the effect of testosterone replacement therapy on correction of metabolic syndrome markers and inflammation in hypogonadal men. They found significant improvements in weight, BMI, WC, and insulin level in the testosterone treatment group compared with the placebo group, and concluded that the decrease

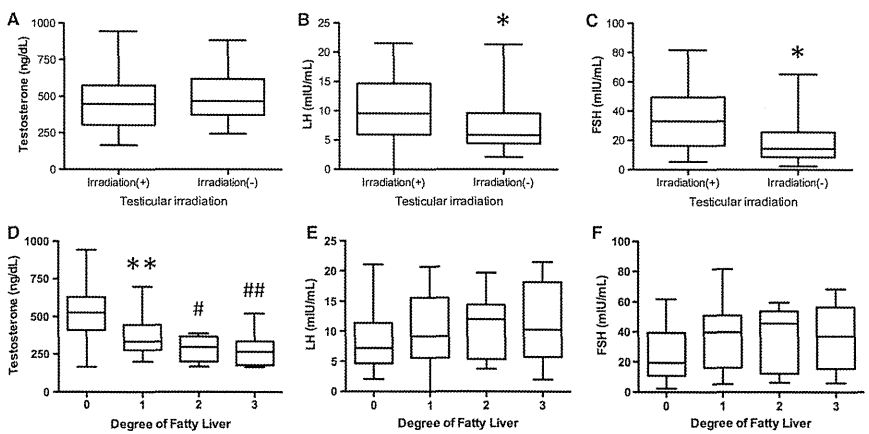

Figure 2. Comparisons of serum testosterone levels (A and D), basal serum LH levels (B and E), and basal serum FSH levels (C and F). The box contains the middle 50th percentile of the value. The lower and upper boundaries of the box indicate the 25th and 75th percentiles, respectively. The bottom and top of the bar show maximum and minimum values, respectively. The degree of fatty liver was classified as follows: 0, absence; 1, mild; 2, moderate; or 3, severe. Significant differences are shown between *testicular irradiation versus no testicular irradiation (P <.0001), **mild fatty liver versus nonfatty liver (P <.001), #moderate fatty liver versus nonfatty liver (P <.001), and ##severe fatty liver versus nonfatty liver (P <.001).

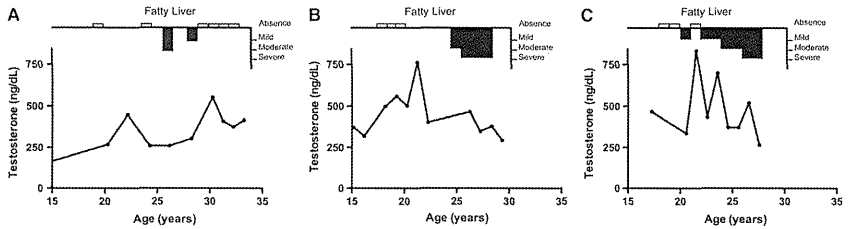

Figure 3. Typical relationship between changes in serum testosterone levels and degree of fatty liver in adult survivors of childhood stem cell transplantation: (A) UPN 011, (B) UPN 044, (C) UPN 212.

in testosterone levels with aging was one of the causes of metabolic syndrome.

Little is known about whether the metabolic syndrome itself may predict the development of hypogonadism, however. One study reported that men with metabolic syndrome had a 2.6-fold increased risk of developing hypogonadism after 11 years [33]. Thus, prevention of abdominal obesity and accompanying metabolic syndrome may reduce the risk of hypogonadism in men. In other studies, weight loss and weight maintenance in men with mainly generalized obesity or abdominal obesity and metabolic syndrome brought about sustained increases in free testosterone levels [34,35]. The prevalence of hypogonadism, as defined by total testosterone levels, decreased from 48% at baseline to 21% after weight loss and 12 months of successful weight maintenance. Weight loss and weight maintenance increased testosterone levels in men with metabolic syndrome after improvement of fatty liver.

This finding of an inverse association between metabolic abnormalities, including insulin resistance, and serum testosterone level is in good agreement with the results of the present study. Fatty liver was more prevalent in patients who received radiation to the brain before undergoing SCT than in those who did not. Although testicular irradiation contributed to damage to the testicular germinal epithelium, testosterone production was maintained during the follow-up period even in patients who received radiation to the testes. Moreover, the degree of fatty liver in patients with insulin resistance was associated with the degree of decreased testosterone secretion. Appropriate exercise and dietary regimens during the follow-up period improved not only insulin resistance, but also fatty liver, and recovery of testosterone secretion followed. Based on these findings, the development and progression of fatty liver in adult survivors of childhood cancer treated with SCT can be considered the cause of, rather than the result of, reduced testosterone levels.

A previous cross-sectional clinical study found an inverse correlation between serum testosterone level and fasting insulin level [36]. Men with insulin resistance, such as those with obesity and those with type 2 DM, have significantly lower testosterone levels than age-matched normal-weight and nondiabetic controls. The mechanism underlying the low testosterone levels associated with insulin resistance in men has not been clarified. Recently, Pitteloud et al [37] reported a positive correlation between testosterone secretion and insulin sensitivity in men. They found a clear association between increased insulin resistance and decreased Leydig cell testosterone secretion in men evaluated by the hyperinsulinemic-euglycemic clamp test. Their findings suggest that the decreased serum testosterone levels in adult survivors of childhood cancer treated with SCT might be explained not only by primary gonadal dysfunction due to the effect of irradiation and/or alkylating agents before SCT but also by the presence of fatty liver and insulin resistance. In addition, several clinical studies have shown significant associations between low SHBG levels and insulin resistance [38] and metabolic syndrome [39]. Shin et al [40] clarified the association between serum SHBG levels and nonalcoholic fatty liver disease in patients with type 2 DM. SHBG levels were lower in patients with high-grade nonalcoholic fatty liver disease than in those without it, and SHBG level was negatively correlated with HOMA-IR score. In the present study, although plasma SHBG level was positively correlated with serum testosterone level, it was not negatively correlated with HOMA-IR, because of an insufficient number of patients for statistical analysis.

A few limitations of the present study need to be considered when interpreting our findings. This longitudinal retrospective study included a small number of patients who underwent SCT in a single institution. In a future study, we plan to analyze the relationship between testosterone level and degree of fatty liver both in patients who underwent SCT and in patients who received chemotherapy only. Our data require confirmation in a large group of patients.

In conclusion, we found significantly higher prevalences of fatty liver and insulin resistance with decreased serum testosterone levels in our patients who underwent SCT to treat childhood cancer than in those who did not. Even those patients who were not overweight or obese were likely to develop fatty liver after SCT. Furthermore, the degree of fatty liver was associated with the degree of reduced serum testosterone level. The incidence of late effects after SCT in our study population increased with follow-up time and did not appear to plateau. We strongly recommend close monitoring of metabolic and endocrine function in adult survivors of childhood SCT in an effort to improve their quality of life.

ACKNOWLEDGMENTS

The authors thank all the medical staff at Tokai University Hospital for providing patient care.

Financial disclosure: This work was supported in part by a research grant from the Foundation for Growth Science. The authors have no conflicts of interest to disclose.

REFERENCES

1. Robison LL, Armstrong GT, Boice JD, et al. The Childhood Cancer Survivor Study: a National Cancer Institute-supported resource for outcome and intervention research. *J Clin Oncol.* 2009;27:2308-2318.
2. Leisenring WM, Mertens AC, Armstrong GT, et al. Pediatric cancer survivorship research: experience of the Childhood Cancer Survivor Study. *J Clin Oncol.* 2009;27:2319-2327.
3. Oeffinger KC, Mertens AC, Sklar CA, et al. Chronic health conditions in adult survivors of childhood cancer. *N Engl J Med.* 2006;355:1572-1582.
4. Ishida Y, Honda M, Ozono S, et al. Late effects and quality of life of childhood cancer survivors, Part 1: impact of stem cell transplantation. *Int J Hematol.* 2010;91:865-876.
5. Ishida Y, Sakamoto N, Kamibeppu K, et al. Late effects and quality of life of childhood cancer survivors, part 2: impact of radiotherapy. *Int J Hematol.* 2010;92:95-104.
6. Nandagopal R, Laverdiere C, Mulrooney D, et al. Endocrine late effects of childhood cancer therapy: a report from the Children's Oncology Group. *Horm Res.* 2008;69:65-74.
7. Oberfield SE, Sklar CA. Endocrine sequelae in survivors of childhood cancer. *Adolesc Med.* 2002;13. 161-169, viii.
8. Ishiguro H, Yasuda Y, Tomita Y, et al. Gonadal shielding to irradiation is effective in protecting testicular growth and function in long-term survivors of bone marrow transplantation during childhood or adolescence. *Bone Marrow Transplant.* 2007;39:483-490.
9. Tomita Y, Ishiguro H, Yasuda Y, et al. High incidence of fatty liver and insulin resistance in long-term adult survivors of childhood SCT. *Bone Marrow Transplant.* 2011;46:416-425.
10. Ishiguro H, Yasuda Y, Tomita Y, et al. Long-term follow-up of thyroid function in patients who received bone marrow transplantation during childhood and adolescence. *J Clin Endocrinol Metab.* 2004;89:5981-5986.
11. Ishiguro H, Yasuda Y, Hyodo H, et al. Growth and endocrine function in long-term adult survivors of childhood stem cell transplant. *Clin Pediatr Endocrinol.* 2009;18:1-14.
12. Bellentani S, Saccoccio G, Masutti F, et al. Prevalence of and risk factors for hepatic steatosis in Northern Italy. *Ann Intern Med.* 2000;132:112-117.
13. Gupte P, Amarapurkar D, Agal S, et al. Non-alcoholic steatohepatitis in type 2 diabetes mellitus. *J Gastroenterol Hepatol.* 2004;19:854-858.
14. Assy N, Kaita K, Mymin D, et al. Fatty infiltration of liver in hyperlipidemic patients. *Dig Dis Sci.* 2000;45:1929-1934.
15. Donati G, Stagni B, Piscaglia F, et al. Increased prevalence of fatty liver in arterial hypertensive patients with normal liver enzymes: role of insulin resistance. *Gut.* 2004;53:1020-1023.
16. Angulo P. Nonalcoholic fatty liver disease. *N Engl J Med.* 2002;346:1221-1231.
17. Volzke H, Aumann N, Krebs A, et al. Hepatic steatosis is associated with low serum testosterone and high serum DHEAS levels in men. *Int J Androl.* 2010;33:45-53.
18. Kaplan SA, Meehan AG, Shah A. The age-related decrease in testosterone is significantly exacerbated in obese men with the metabolic syndrome: what are the implications for the relatively high incidence of erectile dysfunction observed in these men? *J Urol.* 2006;176:1524-1527.
19. Mohr BA, Bhasin S, Link CL, et al. The effect of changes in adiposity on testosterone levels in older men: longitudinal results from the Massachusetts Male Aging Study. *Eur J Endocrinol.* 2006;155:443-452.
20. World Health Organization. Obesity: preventing and managing the global epidemic. Report of a WHO consultation. WHO technical report series 894. Geneva, Switzerland. *World Health Organ Tech Rep Ser.* 2000;894:i-xii, 1-253.
21. Ashwell M, Cole TJ, Dixon AK. Ratio of waist circumference to height is strong predictor of intra-abdominal fat. *BMJ.* 1996;313:559-560.
22. Savva SC, Tornaritis M, Savva ME, et al. Waist circumference and waist-to-height ratio are better predictors of cardiovascular disease risk factors in children than body mass index. *Int J Obes Relat Metab Dis.* 2000;24:1453-1458.
23. Hsieh SD, Yoshinaga H, Muto T. Waist-to-height ratio, a simple and practical index for assessing central fat distribution and metabolic risk in Japanese men and women. *Int J Obes Relat Metab Dis.* 2003;27:610-616.
24. Kojima S, Watanabe N, Numata M, et al. Increase in the prevalence of fatty liver in Japan over the past 12 years: analysis of clinical background. *J Gastroenterol.* 2003;38:954-961.
25. Matsuzawa Y. Metabolic syndrome: definition and diagnostic criteria in Japan [commentary]. *J Atherosclerosis Thromb.* 2005;12:301.
26. Tanner JM, Whitehouse RH. Clinical longitudinal standards for height, weight, height velocity, weight velocity, and stages of puberty. *Arch Dis Child.* 1976;51:170-179.
27. Prader A. Testicular size: assessment and clinical importance. *Triangle.* 1966;7:240-243.
28. Traish AM, Guay A, Feeley R, et al. The dark side of testosterone deficiency, I: metabolic syndrome and erectile dysfunction. *J Androl.* 2009;30:10-22.
29. Stanworth RD, Jones TH. Testosterone in obesity, metabolic syndrome and type 2 diabetes. *Front Horm Res.* 2009;37:74-90.
30. Kapoor D, Goodwin E, Channer KS, et al. Testosterone replacement therapy improves insulin resistance, glycaemic control, visceral adiposity and hypercholesterolaemia in hypogonadal men with type 2 diabetes. *Eur J Endocrinol.* 2006;154:899-906.
31. Jones TH, Arver S, Behre HM, et al. Testosterone replacement in hypogonadal men with type 2 diabetes and/or metabolic syndrome (the TIMES2 study). *Diabetes Care.* 2011;34:828-837.
32. Kalinchenko SY, Tishova YA, Mskhalaya GJ, et al. Effects of testosterone supplementation on markers of the metabolic syndrome and inflammation in hypogonadal men with the metabolic syndrome: the double-blinded placebo-controlled Moscow study. *Clin Endocrinol.* 2010;73:602-612.
33. Laaksonen DE, Niskanen L, Punnonen K, et al. The metabolic syndrome and smoking in relation to hypogonadism in middle-aged men: a prospective cohort study. *J Clin Endocrinol Metab.* 2005;90:712-719.
34. Kaukua J, Pekkarinen T, Sane T, et al. Sex hormones and sexual function in obese men losing weight. *Obes Res.* 2003;11:689-694.

35. Niskanen L, Laaksonen DE, Punnonen K, et al. Changes in sex hormone-binding globulin and testosterone during weight loss and weight maintenance in abdominally obese men with the metabolic syndrome. *Diabetes Obes Metab*. 2004;6:208-215.
36. Simon D, Preziosi P, Barrett-Connor E, et al. Interrelation between plasma testosterone and plasma insulin in healthy adult men: the Telecom Study. *Diabetologia*. 1992;35:173-177.
37. Pitteloud N, Hardin M, Dwyer AA, et al. Increasing insulin resistance is associated with a decrease in Leydig cell testosterone secretion in men. *J Clin Endocrinol Metab*. 2005;90:2636-2641.
38. Sorensen K, Aksglaede L, Munch-Andersen T, et al. Sex hormone-binding globulin levels predict insulin sensitivity, disposition index, and cardiovascular risk during puberty. *Diabetes Care*. 2009;32:909-914.
39. Laaksonen DE, Niskanen L, Punnonen K, et al. Sex hormones, inflammation and the metabolic syndrome: a population-based study. *Eur J Endocrinol*. 2003;149:601-608.
40. Shin JY, Kim SK, Lee MY, et al. Serum sex hormone-binding globulin levels are independently associated with nonalcoholic fatty liver disease in people with type 2 diabetes. *Diabetes Res Clin Pract*. 2011;94:156-162.

ASBMT
American Society for Blood and Marrow Transplantation

High Incidence of Radiation-Induced Cavernous Hemangioma in Long-Term Survivors Who Underwent Hematopoietic Stem Cell Transplantation with Radiation Therapy during Childhood or Adolescence

Takashi Koike,[1] Noriharu Yanagimachi,[2] Hiroyuki Ishiguro,[1] Hiromasa Yabe,[3] Miharu Yabe,[4] Tsuyoshi Morimoto,[1] Takashi Shimizu,[2] Hiromitsu Takakura,[1] Shunichi Kato[3]

Radiation-induced cavernous hemangioma (RICH) is a late complication of cerebral radiation therapy. Long-term survivors of hematopoietic stem cell transplantation (HSCT) who underwent radiation therapy could be at increased risk for RICH. We investigated records of 68 patients who underwent HSCT during childhood or adolescence and were assessed by magnetic resonance imaging (MRI), including T2*-weighted imaging of the brain, annually for 5 years over a range of 6 to 29 years after HSCT. We developed a scoring and grading system for RICH to monitor the process and the progress of radiologic changes. Among the 68 patients investigated, 28 (41.2%) were diagnosed with CH. All 28 patients had received total body irradiation as a conditioning treatment for HSCT and/or cranial radiation therapy before HSCT as part of the treatment of their primary disease. RICH was diagnosed in none of the patients who did not receive radiation (n = 19), in 46.2% of those who received 6 to 12 Gy (n = 39), and in all of those who received 18 to 36 Gy (n = 10). Total RICH scores were correlated with higher radiation doses. Careful and long-term evaluation with MRI, including T2*-weighted imaging, is necessary for HSCT recipients who received radiation therapy before and/or during HSCT.

Biol Blood Marrow Transplant ■: 1-9 (2012) © 2012 *American Society for Blood and Marrow Transplantation*

KEY WORDS: Cavernous hemangioma, Radiation, Late effect, T2*-weighted magnetic resonance imaging, Score

INTRODUCTION

Hematopoietic stem cell transplantation (HSCT) has been widely applied to treat a variety of malignant and nonmalignant diseases in childhood. Advances in transplantation practices and supportive care have led to improved outcomes and have resulted in an increasing number of long-term HSCT survivors [1-3]. The overall survival rate after HSCT in childhood is now >50%, and more than 5,000 childhood HSCT recipients are estimated to be currently surviving long-term in Japan [4]. However, childhood and adulthood survivors experience morbidity, which is generally related to the treatment they received to cure their original disease rather than to the disease itself, and treatment-related morbidity is extraordinarily diverse [5]. HSCT survivors are at significant risk of developing late complications after successful transplantation during childhood [6]. In particular, radiation therapy may be a cause of later complications, such as secondary neoplasm [6], growth failure [7], thyroid dysfunction [8], and gonadal dysfunction [9].

Cranial radiation therapy (CRT) has been an integral part of the treatment of patients with cranial tumors, other solid tumors of the head, and disorders with central nervous system involvement, as well as to prevent central nervous system relapse in acute leukemia. Known late complications of radiation therapy include not only endocrine dysfunction, cognitive deterioration, and secondary neoplasm, but also the risk of developing cavernous hemangioma (CH). The prevalence of CH or cavernous malformation was found to be as high as 0.5% in a large prospective cohort from the general population without radiation exposure [10]. Although these malformations were initially thought to be congenital, in 1994, Ciricillo et al [11] reported seven patients with intracerebral cavernoma as a possible consequence of radiation, and since then, another 84 cases and reviews have been described [12].

The literature suggests that radiation doses >30 Gy are associated with a shorter latency period and that younger age at the time of radiation exposure is a risk factor for developing radiation-induced cavernous hemangioma (RICH) [13]. However, despite the increasing number of reported cases, the mechanisms of CH formation after radiation are complex, and the impacts of radiation dose, sex, and age at the time of radiation therapy remain poorly understood. A longitudinal study investigating the relationship between HSCT and developing RICH in survivors of childhood HSCT has yet to be published. To evaluate the prevalence of RICH, we performed a longitudinal retrospective study of adult survivors of childhood HSCT at a single institution.

From the [1]Department of Pediatrics; [2]Radiology; [3]Cell Transplantation and Regenerative Medicine; and [4]Laboratory Medicine, Tokai University School of Medicine, Kanagawa, Japan.

Financial disclosure: See Acknowledgments on page 8.

Correspondence and reprint requests: Shunichi Kato, Department of Cell Transplantation and Regenerative Medicine, Tokai University School of Medicine, 143 Shimokasuya, Isehara, Kanagawa 259-1193, Japan (e-mail: skato@is.icc.u-tokai.ac.jp).

Received September 21, 2011; accepted December 21, 2011

1083-8791/$36.00
doi:10.1016/j.bbmt.2011.12.582

PATIENTS AND METHODS

Patients

We investigated 147 patients who underwent HSCT during childhood or adolescence at Tokai University Hospital between March 1982 and July 2000 and had annual follow-up after HSCT. Inclusion criteria were survival for at least 10 years after HSCT, no previous history of brain disease before HSCT, and annual brain magnetic resonance imaging (MRI) studies between April 1, 2006, and July 31, 2011.

Among the 147 patients, 68 (35 males and 33 females) visited Tokai University Hospital annually throughout the follow-up period and were enrolled in this study. The remaining 79 patients were followed up at Tokai University Hospital initially but then received continuing follow-up at their referring hospitals without T2*-weighted MRI; these patients were excluded from this study.

The median age of the 68 patients at HSCT was 7 years (range, 0-24 years) and that at the last evaluation was 28 years (range, 14-43 years). The median follow-up duration after HSCT was 19 years (range, 10-28 years). Patient characteristics are summarized in Table 1. Written informed consent was obtained from all patients and/or parents. The study was approved by Tokai University's Clinical Research Review Committee.

Transplantation Procedure

In addition to conventional chemotherapy, nine patients with acute lymphoblastic leukemia (ALL) and one patient with non-Hodgkin lymphoma (NHL) received prophylactic CRT (24 Gy in one patient and 18 Gy in nine patients) between 1 year and 9 years before HSCT. In 54 patients, the consitioning regimen comprised irradiation with or without cyclophosphamide and/or other drugs. Between 6 and 12 Gy of total body irradiation (TBI) for malignant diseases was given in 3 to 6 fractions, and 6 to 8 Gy of thoracoabdominal irradiation for nonmalignant diseases was given in three or four fractions. The remaining 14 patients received conditioning without irradiation.

The method of TBI delivery remained constant during the period when those patients underwent HSCT, whereas the method of CRT delivery varied among the institutions in which those patients were treated initially. Prophylaxis against graft-versus-host disease varied during the study period and used methotrexate, cyclosporine, or a combination of the two.

Brain MRI

The radiologic diagnosis of CH was made based on MRI findings, including gradient-echo sequence (T2*-weighted imaging) and contrast MRI with gadolinium chelates, performed annually for 6 to 29 years after HSCT. MRI was done using mainly a 1.5-T and occasionally a 3-T superconducting MRI system. Typical appearance on T2-weighted MRI was a peripheral rim of hypointense hemosiderin surrounding a central core of heterogeneous reticulated signal, often described as "popcorn-like." The hypointense ring may represent repeated subclinical intralesional and perilesional hemorrhages leading to ferritin deposition secondary to erythrocyte breakdown [14]. In particular, T2*-weighted imaging of the brain is highly sensitive for the detection of small CH.

CH Score

The patients were evaluated for CH number, size, and distribution and for annual changes in these parameters. We developed a CH scoring system based on MRI findings to monitor the process and the progress of radiologic changes. CH size <3 mm was defined as score1 (1 point), CH size 3 to 5 mm as score2 (2 points), CH size 6 to 8 mm as score3 (3 points), and CH size ≥9 mm as score4 (4 points) (Figure 1).

CH Grade

The magnitude of CH was graded according to total CH score and the presence of mass effect as grade 0, total score 0; grade I, total score 1-4; grade II, total score 5-9; grade III, total score ≥10; or grade IV, total score ≥5 and mass effect present.

Statistical Analysis

Because the data had a skewed distribution, values are presented as median and range. Differences in eight variables—sex, age at HSCT, age at first radiation therapy, age at latest MRI, age at diagnosis of CH, original disease, radiation dose to the head, and type of transplantation—among groups were analyzed by the Pearson χ^2 test or Fisher exact test. The

Table 1. Patient Characteristics

	Total	Groups According to Total Cranial Radiation Dose		
		A (0 Gy)	B (6-12 Gy)	C (18-36 Gy)
Number of patients	68	19	39	10
Females/males, n	33/35	6/13	21/18	6/4
Primary disease, n				
Malignant diseases				
Acute lymphoblastic leukemia	18	0	9	9
Acute myelogenous leukemia	11	0	11	0
Chronic myelogenous leukemia	5	1	4	0
Juvenile myelomonocytic leukemia	1	0	1	0
Myelodysplastic syndrome	2	0	2	0
Non-Hodgkin lymphoma	4	0	3	1
Neuroblastoma	2	0	2	0
Yolk sac tumor	1	0	1	0
Nonmalignant diseases				
Severe aplastic anemia	10	6	4	0
Others	14	12	2	0
Autologous/allogeneic HSCT, n	7/61	0/19	6/33	1/9
Age at HSCT, years, median (range)	7 (0-24)	5 (1-12)	9 (0-24)	10 (4-19)
Age at first irradiation, years, median (range)	8 (0-24)		9 (0-24)	6 (0-17)
Age at latest MRI, years, median (range)	28 (14-43)	24 (12-33)	29 (16-43)	28.5 (21-37)
Follow-up after HSCT, years, median (range)	19 (10-28)	16 (10-23)	20 (11-28)	18 (16-21)

Mann-Whitney *U* test and the Kruskal-Wallis test were used to compare differences between groups. A Kaplan-Meier survival curve was constructed to assess the probability of CH incidence, and the log-rank test was used to compare probabilities. In multivariate analyses, outcome comparisons were adjusted with Cox proportional hazards models and tested by the likelihood ratio test. All statistical analyses were performed with SPSS version 19. A P value <.05 was considered statistically significant.

RESULTS

Incidence of CH

CH was diagnosed in 28 of the 68 patients (41.2%) by MRI during the follow-up period (Table 2). The probability of developing CH at 25 years after HSCT was 61.5% ± 9.1% by the Kaplan-Meier method (Figure 2A). The median age at diagnosis of CH was 27 years (range, 11-40 years). The median age at HSCT was 9.5 years (range, 1-22 years), and the median age at first irradiation treatment in the patients diagnosed with CH was 7.5 years (range, 0-22 years).

Incidence and probability were further analyzed according to several variables to evaluate risk factors for CH (Table 2). Gender, type of transplantation and age at the first irradiation did not give statistically significant differences in frequency or in probability of CH. However, compared with patients with nonmalignant diseases, those with malignant diseases in which HSCT was indicated had a significantly higher frequency of CH (59.1 versus 8.3%; $P < .001$) and a significantly higher probability of developing CH (75.6% ± 8.6% versus 6.2% ± 6.1%; $P < .001$).

Age at HSCT showed a marginally significant effect. Patients who underwent HSCT at age ≥15 years had a slightly higher probability of developing CH than did younger patients (56.8% ± 12.8% versus 72.1% ± 11.3%; $P < .05$). The mean total cranial radiation dose was 8.8 ± 8.4 Gy in patients aged 0 to 9 years and 12.8 ± 8.5 Gy in those aged ≥10 years ($P = .058$).

The patients were divided into three groups according to total cranial radiation dose: group A, none (n = 19); group B, 6 to 12 Gy (n = 39); and group C, 18 to 36 Gy (n = 10). CH was not detected in any of the group A patients but was found in 46.2% of the group B patients and in 100% of the group C patients; the intragroup differences were highly significant ($P < .001$) (Table 2). The probability of CH was 0% in group A, 62.0% ± 10.1% in group B, and 100% in group C ($P < .001$) (Table 2 and Figure 2B).

The results of Cox multivariate regression analysis for developing CH are presented in Table 3. Of the covariates shown to be significant in univariate analysis, only cranial radiation dose was found to be significantly associated with CH risk ($P < .001$).

CH score	CH size
1	<3mm
2	3mm≤, <6mm
3	6mm≤, <9mm
4	9mm≤

CH grade	Total CH score
0	0
I	1-4
II	5-9
III	10-
IV	Mass effect and CH score ≥ 5

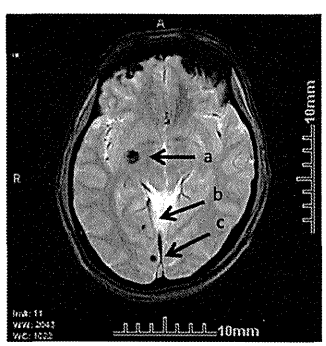

Figure 1. CH scoring and grading system. This example case has a total CH score of 6 [a(score 3) + b(score 1) + c(score 2)] and CH grade II.

Table 2. Univariate Analysis of the Incidence of CH with the Frequency and Probability of Developing CH by the Kaplan-Meier Test

Category	N	CH Incidence, n (%)	P Value[a]	Probability, %	P Value[b]
Total	68	28 (41.2)		61.5 ± 9.1	
Sex					
Female	33	16 (48.5)	NS	70.9 ± 11.2	NS
Male	35	12 (34.3)		75.6 ± 18.4	
Primary disease					
Malignant	44	26 (59.1)	<.001	75.6 ± 8.6	<.001
Nonmalignant	24	2 (8.3)		6.2 ± 6.1	
Type of transplantation					
Autologous	7	4 (57.1)	NS	61.9 ± 19.9	NS
Allogeneic	61	24 (39.3)		61.7 ± 10.8	
Age at HSCT, years					
<10	41	14 (34.2)	NS	56.8 ± 12.8	<.05
≥10	27	14 (51.9)		72.1 ± 11.3	
Age at first radiation, years					
<10	28	16 (57.1)	NS	68.1 ± 11.0	NS
≥10	21	12 (57.1)		75.8 ± 11.8	
Total cranial radiation dose, Gy					
0	19	0 (0)	<.001	0	<.001
6-12	39	18 (46.2)		62.0 ± 10.1	
18-30	10	10 (100)		100	

NS indicates not significant.
[a]Pearson's χ square test or Fisher exact test.
[b]Log-rank test (Kaplan-Meier).

CH Score and Grade

In the 28 patients with CH, the total CH score at the latest MRI ranged from 1 to 19 points (median, 5 points). The total number of CH lesions in these patients was 115, including 75 lesions with a CH score of 1, 27 with a CH score of 2, four with a CH score of 3, and four with a CH score of 5. Only 21 of the 115 lesions that were identified by T2*-weighted MRI (18.3%) were visible on conventional T2-weighted MRI. In particular, conventional T2-weighted MRI could identify all nine lesions with a CH score of 3 or 4 but none of lesions with a CH score of 1 or 2.

The most common location of CH was supratentorial (n = 102; 88.7%), particularly in the

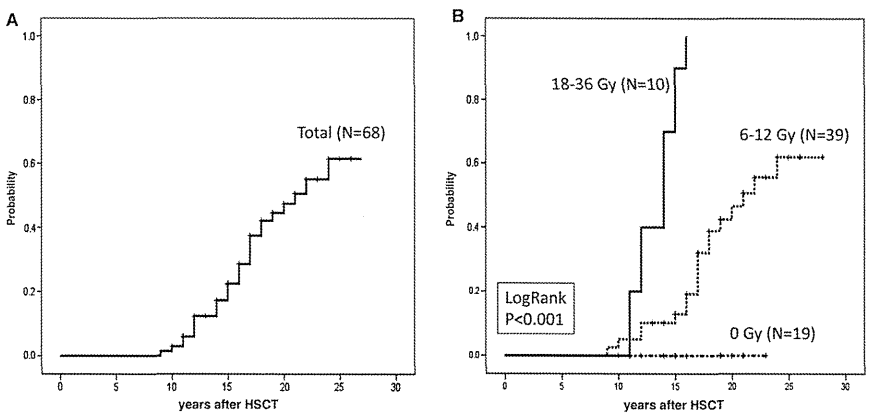

Figure 2. Probabilty of developing CH after HSCT. (A) The probability of developing CH in the 68 study patients was 61.5% ± 9.1% at 25 years after HSCT. (B) Based on total cranial radiation dose, the probability was 0% in the patients who did not receive irradiation to the head before and/or during the conditioning treatment for HSCT, 62.0% ± 10.1% in those with a total cranial radiation dose of 6 to 12 Gy, and 100% in those with a total dose of 18 to 36 Gy. These differences are highly significant ($P < .001$).

Table 3. Cox Multivariate Regression Analysis for Developing CH

	HR[a]	95% CI	P Value
Disease (malignant versus nonmalignant)	2.02	0.45-9.05	.360
Age at transplantation (<10 years versus ≥10 years)	1.37	0.62-3.02	.435
Cranial radiation dose (0 versus 6-12 versus 19-36 Gy)	10.02	3.65-27.49	<.001

[a]Hazard ratio.

frontal and parietal lobes, and CH was prevalent in subcortical and deep white matter (Table 4). Only 13 infratentorial and basal ganglia lesions (11.3%) were identified, most of which were in the cerebellum (10 of 13; 76.9%) (Table 5).

A significant correlation was found between the latest total CH score and the total cranial radiation dose (Figure 3). Neither age at HSCT nor age at the first irradiation treatment were correlated with CH score (data not shown). CH grade was 0 in 40 patients, I in 14 patients, II in eight patients, III in four patients, and IV in one patient.

Changes in CH Score During the 5-Year Observation Period

CH was identified on the initial MRI in 22 patients, and was newly identified in six patients during the 5-year observation period. Mixed high and low

Table 4. Supratentorial Localization of CH Lesions

CH Score	Frontal Lobe	Temporal Lobe	Parietal Lobe	Occipital Lobe	Total
Cerebral cortex					
1	1	2	3	3	9
2	3		2	1	6
3					
4		1			1
Subtotal	4	3	5	4	16
Subcortical white matter					
1	15	5	12	3	35
2	6		5		11
3			1		1
4		1			1
Subtotal	21	6	18	3	48
Deep white matter					
1	12	3	7	2	24
2	1	1	1	1	4
3					
4					
Subtotal	13	4	8	3	28
Periventricular white matter					
1	4		2	1	7
2	2				2
3	1				1
4					
Subtotal	7	0	2	1	10
Total					
1	32	10	24	9	75
2	12	1	8	2	23
3	1		1		2
4		2			2
Total	45	13	33	11	102

Table 5. Localization of Infratentorial and Basal Ganglia CH Lesions

CH Score	Basal Ganglia	Thalamus	Midbrain	Pons	Cerebellum	Total
1		1		1	2	4
2					4	4
3					2	2
4	1				2	3
Total	1	1	0	1	10	13

signals on T1- and T2-weighted imaging with or without surrounding edema that had been absent in previous MRI images were newly identified in six patients.

Changes in total CH score according to time after initial brain irradiation treatment are shown in Figure 4. Over the 5-year observation period, 23 of the 28 patients (82.1%) had an increase in total CH score, by 1-10 points. Three patients exhibited a transient increase in total CH score, possibly reflecting artifacts of T2*-weighted MRI. In terms of grading classification, three patients progressed from grade I to grade II, and three progressed from grade II to grade III during the 5-year observation period.

Clinical Symptoms

Two patients experienced episodes of vertigo and headache and bleeding from CH at the cerebellum that was diagnosed by conventional MRI at other hospitals. CH grade was I (total score 4) in one of these patients and III (total score 15) in the other. One patient had frequent headaches and CH (grade III; total score 15) detected just before enrolling in this study. Another patient had hand numbness and was diagnosed with CH (grade IV, total score 6) at our hospital, where MRI and computed tomography (CT) scan revealed a giant CH in the right basal ganglia (Figure 5). Consultation with a neurosurgeon resulted in periodical MRI examinations and careful follow-up. Exacerbation of symptoms has not been observed during the subsequent 5 years, but the patient's total CH score increased from 6 to 7 because of a new lesion found in the left frontal lobe. All other patients with CH lesions detected in this study were asymptomatic throughout the follow-up period.

Venous Angioma

Venous malformation or angioma was not detected on contrast MRI with gadolinium-chelates in any of the patients with or without CH changes.

DISCUSSION

RICH of the brain was first recognized as a late effect of radiation therapy for brain tumors using high-dose irradiation (50-60 Gy). This effect is commonly seen in children treated with radiation therapy for reasons other than brain tumors. Progress in diagnostic

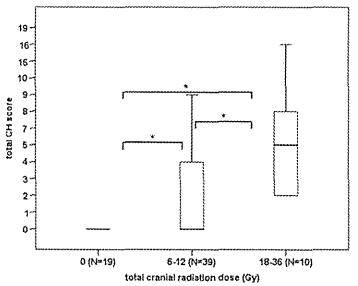

Figure 3. Total CH scores according to total cranial radiation dose before and/or during conditioning treatment for HSCT. Total CH scores between 0 Gy and 6-12 Gy, between 0 Gy and 18-36 Gy, and between 6-12 Gy and 18-36 Gy were statistically significantly different. *$P < .001$, Mann-Whitney U test.

techniques, such as MRI, has contributed to the early detection of RICH. However, little is known about the incidence, dose relationship, localization, natural course, and clinical symptoms in HSCT recipients, in whom radiation is often used as a part of chemotherapy for leukemia or as TBI in conditioning.

Strenger et al [15] reported that eight of 171 pediatric patients who underwent cranial radiation at 9 to 85.6 Gy at age 10.5 months to 38.5 years (median, 8.3 years) developed CH at 2.9 to 18.4 years after irradiation, with a cumulative incidence of 6.74% at 20 years after radiation therapy. In that study, CT or conventional MRI without T2*-weighted imaging was used to diagnose CH. Koike et al [16] reported that 18 of 90 children (20%) who had received 18 to 66 Gy of cranial radiation at age 0-17 years (mean, 7.2 ± 4.5 years) developed CH at 2 to 10 years after the initial irradiation.

In the present study, 28 of 68 long-term adult survivors of childhood HSCT (41.2%) were diagnosed with CH, and the probability of developing CH by 25 years after HSCT was 61.5% ± 9.1%. Given that the incidence of intracranial cavernous malformations is approximately 0.5% in the general population, the frequency and probability in our series apparently exceed this range. Because CH was not found in patients who had not received radiation to the head before and/or during the conditioning regimen for HSCT, radiation was considered the cause of CH in those survivors.

CH was found in no patients who did not receive cranial radiation (n = 19), in 46.2% of those who received 6 to 12 Gy (n = 39), and in 100% of those who received 18 to 36 Gy (n = 10). Thus, 6 to 12 Gy might be considered the threshold level for development of RICH, and higher radiation dose was significantly associated with a higher frequency of RICH.

Younger age has been reported as a risk factor for RICH by several authors. However, this association with younger age was not found in the present study, and CH developed at a slightly higher frequency in children aged >15 years at the time of radiation therapy. This higher incidence in the oldest age group was considered related to the higher total cranial radiation dose received by this group.

Naturally occurring CH is known to be associated with developmental venous malformation (DVM) or angioma (DVA), which is usually occult and detected during surgery or at autopsy, with a crude detection rate of 0.43 per 100,000 adults per year [17]. Abdulrauf et al [18] reported DVM in 24% of patients with CH, and DVA is reportedly associated with cavernous malformation in 8% to 33% of cases [19]. DVA was not found in our patients on contrast MRI; susceptibility-weighted MRI might be more sensitive for detecting DVA. Thus, the causative association of DVM and CH is less likely in our patients.

Cox multivariate regression analysis identified cranial radiation dose as the sole factor affecting the development of CH in our analysis. However, other factors, such as intrathecal therapy or certain chemotherapies, might have contributed to the development of late changes in neurologic function and may be related to the imaging changes to some extent. We could not analyze such factors, however, because we could not collect all of these data from the referring hospitals.

T2*-weighted MRI was sensitive and useful in the early detection of CH. Maeda et al [20] judged

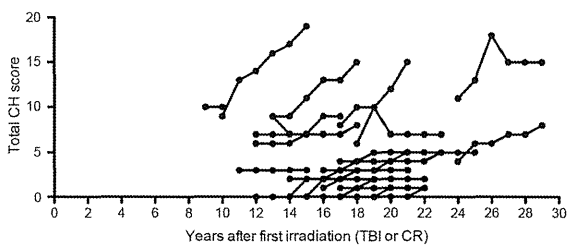

Figure 4. Changes in total CH scores during the 5-year observation period in the patients who developed RICH.

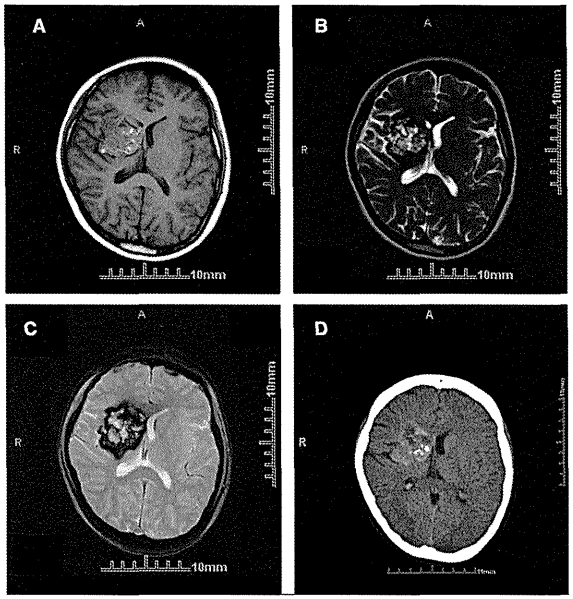

Figure 5. MRI and CT images in a patient with a giant CH. (A) T1-weighted MRI. (B) T2-weighted MRI. (C) T2*-weighted MRI. (D) CT.

T2*-weighted MRI superior to conventional T2-weighted MRI in detecting the number and distribution of lesions in CH. In our analysis, small lesions were identified only on T2*-weighted imaging, not on conventional T2-weighted imaging, likely contributing to the higher incidence in the present study compared with previous reports.

The onset of CH detected by T2*-weighted MRI ranged from 9 to 24 years after HSCT and also from 9 to 24 years after the first radiation treatment, whereas diagnosis of CH by conventional T2-weighted MRI was delayed or not possible in most cases. Because CH changes were already present in most survivors at the time of initial MRI, actual onset was considered to be earlier. Thus, the present study has a limited ability to precisely detect the onset of RICH.

As in previous reports of RICH, the most common localization of hemangioma was supratentorial, particularly in the subcortical and deep white matter. Infratentorial lesions were found predominantly in the cerebellum, which might have caused clinical symptoms, such as vertigo or headache, in a few patients.

The CH scoring system that we have developed is useful for quantifying lesions and evaluating changes occurring during the follow-up period. Increased CH scores were seen in 23 of 28 patients (82.1%) during the 5-year observation period. Thus, this study reveals details of the course and speed of CH growth through annual follow-up examinations. The use of this scoring method could also provide insight into the pathogenesis and natural course of RICH, although the method's clinical relevance remains uncertain given the small number of patients and short follow-up period of the present study.

In general, RICH lesions neither disappear nor diminish over their natural course. However, a decrease in CH score after a transient increase was seen in three patients during the study period. This transient increase in CH score was considered related to an artifact of T2*-weighted MRI. Evaluation by single-time point MRI may carry a risk of overestimation, and thus careful evaluation by serial MRI over sufficient intervals is necessary.

Despite the progression of some CH lesions, most patients remained asymptomatic, as in previous reports. Newly recognized signal changes on T1- and T2-weighted MRI with or without surrounding edema of preexisting CH are considered to reflect bleeding episodes during the intervals between examinations, and repeated bleeding may finally form a mass lesion. Symptomatic bleeding may occur with or without triggers that cause a rapid increase in blood pressure,

however. Pregnancy and labor are known risk factors for such bleeding [21], probably because the angiogenic process is initiated by growth factors, such as vascular endothelial growth factor, basic fibroblast growth factor, and placental growth factor [22]. We treated a case of seizure caused by CH bleeding during labor in a 31-year-old female who had a history of cranial radiation of 18 Gy for acute lymphoblastic leukemia in childhood. Her CH grade was IV with a mass effect at the right parahippocampal gyrus, and her total CH score was 23. This patient was not included in the present study because she had no history of HSCT.

We suggest that MRI, including T2*-weighted imaging, should be routinely and serially performed over the long term in those who have received radiation to the head during childhood or adolescence. Attention should also be given to patients in whom RICH was identified, especially those with grade III/IV CH, regardless of the localization of lesions, or those with grade I/II CH with infratentorial lesions, given that infratentorial CH is more closely associated with symptomatic bleeding compared with supratentorial CH [23,24]. Information on the presence of RICH will aid accurate diagnosis in those survivors and facilitate proper management in the event of clinical bleeding episodes. Surgical indications in those with repeated bleeding episodes and progressive neurologic symptoms should be discussed with a neurosurgeon.

Routine and serial MRI is useful for early detection of other well-recognized brain imaging changes, such as mineralizing microangiopathy, leukoencephalopathy, and brain tumors [25]. Meningioma was detected in eight patients with cranial radiation (five with RICH and three without RICH), and oligoastrocytoma was detected in one patient with cranial radiation and RICH and will be reported separately.

Although we have clarified the high incidence and the importance of RICH in adult long-term survivors of HSCT performed during childhood in a single-center study, the mechanisms of RICH remain unknown. Retrospective and multicenter studies using sensitive T2*-weighted MRI on long-term survivors of childhood cancer who received radiation to the skull should be planned to confirm the actual incidence of RICH in a larger population. Prospective and long-term studies on those who received radiation to the head during treatment are needed to examine the onset and natural course of RICH.

In conclusion, because all of our patients with CH had a history of radiation therapy to the brain, and because none of the patients who did not receive radiation therapy developed CH, the cause of CH in those adult survivors of childhood HSCT was considered to be radiation. We found a dose-reponse relationship between total cranial radiation and the development of CH and determined that the radiation dose of 6 to 12 Gy commonly used in patients undergoing HSCT could cause RICH. Careful and long-term evaluation with MRI, including T2*-weighted imaging, is strongly recommended in HSCT recipients who received radiation therapy before and/or during HSCT. This is the first report of a high prevalence of RICH among long-term HSCT survivors, in which radiologic changes were quantitatively and longitudinally evaluated by annual MRI, including T2*-weighted imaging.

ACKNOWLEDGMENTS

We thank the medical staff at Tokai University Hospital for patient care and examination. We appreciate the excellent support of Professor Hiroyuki Kobayashi for statistical analysis.

Authorship Statement: Shunichi Kato designed research and followed up with HSCT survivors. Takashi Koike, Hiroyuki Ishiguro, and Shunichi Kato analyzed data and wrote the manuscript. Noriharu Yanagimachi diagnosed CH by MRI. Hiromasa Yabe, Miharu Yabe, Tsuyoshi Morimoto, Takashi Shimizu, and Hiromitsu Takakura provided clinical information.

Financial disclosure: The authors have no conflicts of interest to disclose.

REFERENCES

1. Robison LL, Armstrong GT, Boice JD, et al. The Childhood Cancer Survivor Study: a National Cancer Institute–supported resource for outcome and intervention research. *J Clin Oncol.* 2009;27:2308-2318.
2. Leisenring WM, Mertens AC, Armstrong GT, et al. Pediatric cancer survivorship research: experience of the Childhood Cancer Survivor Study. *J Clin Oncol.* 2009;27:2319-2327.
3. Oeffinger KC, Mertens AC, Sklar CA, et al. Chronic health conditions in adult survivors of childhood cancer. *N Engl J Med.* 2006;355:1572-1582.
4. Committee for Nationwide Survey Data Management. Transplant activity report. In: Imamura M, Hara M, Sakamaki H, Kato K, Mitamura M, Tanaka J, Hiraoka A, Adachi S, Kato S, Yabe H, Kawa K, Morishima Y, Takanashi M, Nagamura T, Suzuki R, editors. *Annual Report of Nationwide Survey 2010. Monograph*, Vol.29. Nagoya: The Japan Society for Hematopoietic Cell Transplantation; 2011. p. 3-80.
5. Ishida Y, Honda M, Ozono S, et al. Late effects and quality of life of childhood cancer survivors, part 1: impact of stem cell transplantation. *Int J Hematol.* 2010;91:865-876.
6. Hudson MM, Mulrooney DA, Bowers DC, et al. High-risk populations identified in Childhood Cancer Survivor Study investigations: implications for risk-based surveillance. *J Clin Oncol.* 2009;27:2405-2414.
7. Ishiguro H, Yasuda Y, Hyodo H, et al. Growth and endocrine function in long-term adult survivors of childhood stem cell transplant. *Clin Pediatr Endocrinol.* 2009;18:1-14.
8. Ishiguro H, Yasuda Y, Tomita Y, et al. Long-term follow-up of thyroid function in patients who received bone marrow transplantation during childhood and adolescence. *J Clin Endocrinol Metab.* 2004;89:5981-5986.
9. Ishiguro H, Yasuda Y, Tomita Y, et al. Gonadal shielding to irradiation is effective in protecting testicular growth and function in long-term survivors of bone marrow transplantation during

childhood or adolescence. *Bone Marrow Transplant*. 2007;39: 483-490.
10. Kim DS, Park YG, Choi JU, et al. An analysis of the natural history of cavernous malformations. *Surg Neurol*. 1997;48:9-17.
11. Ciricillo SF, Cogen PH, Edwards MS. Pediatric cryptic vascular malformations: presentation, diagnosis and treatment. *Pediatr Neurosurg*. 1994;20:137-147.
12. Keezer MR, Del Maestro R. Radiation-induced cavernous hemangiomas: case report and literature review. *Can J Neurol Sci*. 2009;36:303-310.
13. Heckl S, Aschoff A, Kunze S. Radiation-induced cavernous hemangiomas of the brain. *Cancer*. 2002;94:3285-3291.
14. Liu Y, Preston R, Thomas SM, et al. Cerebral cavernoma: an emerging long-term consequence of external beam radiation in childhood. *Clin Endocrinol*. 2010;73:555-560.
15. Strenger V, Sovinz P, Lackner H, et al. Intracerebral cavernous hemangioma after cranial irradiation in childhood: incidence and risk factors. *Strahlenther Onkol*. 2008;184:276-280.
16. Koike S, Aida N, Hata M, et al. Asymptomatic radiation-induced telangiectasia in children after cranial irradiation: frequency, latency, and dose relation. *Radiology*. 2004;230:93-99.
17. Al-Shahi R, Bhattacharya JJ, Currie DG, et al. Prospective, population-based detection of intracranial vascular malformations in adults: the Scottish Intracranial Vascular Malformation Study (SIVMS). *Stroke*. 2003;34:1163-1169.
18. Abdulrauf SI, Kaynar MY, Awad IA. A comparison of the clinical profile of cavernous malformations with or without associated venous malformations. *Neurosurgery*. 1999;44:41-46.
19. Rabinov JD. Diagnostic imaging of angiographically occult vascular malformations. *Neurosurg Clin North Am*. 1999;10: 419-432.
20. Maeda K, Terashima T, Kawai H, et al. T2*-weighted MR images of a patient with familial cerebral cavernous malformation. *Intern Med*. 2007;46:541-542.
21. Savi-Abbasi S, Feiz-Erfan I, Spetzler R, et al. Hemorrhage of cavernous malformations during pregnancy and in the peripartum period: causal or coincidence? *Neurosurg Focus*. 2006;21:E12.
22. Zygmunt M, Herr F, Munstedt K, et al. Angiogenesis and vasculogenesis in pregnancy. *Eur J Obstet Gynecol Reprod Biol*. 2003; 110(suppl 1):S10-S18.
23. Abla AA, Turner JD, Mitha AP, et al. Surgical approaches to brainstem cavernous malformations. *Neurosurg Focus*. 2010; 29:E8.
24. Porter PJ, Willinsky RA, Harper W, et al. Cerebral cavernous malformations: natural history and prognosis after clinical deterioration with or without hemorrhage. *J Neurosurg*. 1997;87: 190-197.
25. Vazques E, Lucaya J, Castellote A, et al. Neuroimaging in pediatric leukemia and lymphoma: differential diagnosis. *Radiographics*. 2002;22:1411-1428.

J Clin Immunol
DOI 10.1007/s10875-011-9638-z

Clinical and Genetic Characteristics of XIAP Deficiency in Japan

Xi Yang · Hirokazu Kanegane · Naonori Nishida · Toshihiko Imamura · Kazuko Hamamoto · Ritsuko Miyashita · Kohsuke Imai · Shigeaki Nonoyama · Kazunori Sanayama · Akiko Yamaide · Fumiyo Kato · Kozo Nagai · Eiichi Ishii · Menno C. van Zelm · Sylvain Latour · Xiao-Dong Zhao · Toshio Miyawaki

Received: 26 July 2011 / Accepted: 14 December 2011

Abstract Deficiency of X-linked inhibitor of apoptosis (XIAP) caused by *XIAP/BIRC4* gene mutations is an inherited immune defect recognized as X-linked lymphoproliferative syndrome type 2. This disease is mainly observed in patients with hemophagocytic lymphohistiocytosis (HLH) often associated with Epstein–Barr virus infection. We described nine Japanese patients from six unrelated families with XIAP deficiency and studied XIAP protein expression, *XIAP* gene analysis, invariant natural killer T (iNKT) cell counts, and the cytotoxic activity of $CD8^+$ alloantigen-specific cytotoxic T lymphocytes. Of the nine patients, eight patients presented with symptoms in infancy or early childhood. Five patients presented with recurrent HLH, one of whom had severe HLH and died after cord blood transplantation. One patient presented with colitis, as did another patient's maternal uncle, who died of colitis at 4 years of age prior to diagnosis with XIAP deficiency. Interestingly, a 17-year-old patient was asymptomatic, while his younger brother suffered from recurrent HLH and EBV infection. Seven out of eight patients showed decreased XIAP protein expression. iNKT cells from patients with XIAP deficiency were significantly decreased as compared with age-matched healthy controls. These results in our Japanese cohort are compatible with previous studies, confirming the clinical characteristics of XIAP deficiency.

Keywords X-linked lymphoproliferative syndrome · X-linked inhibitor of apoptosis · Epstein–Barr virus · hemophagocytic lymphohistiocytosis · invariant natural killer T cell

Abbreviations

BIR	Baculovirus IAP repeat
CTL	Cytotoxic T lymphocyte
HSCT	Hematopoietic stem cell transplantation
HLH	Hemophagocytic lymphohistiocytosis
IAP	Inhibitor of apoptosis
LCL	Lymphoblastoid cell line
MMC	Mitomycin C
mAb	Monoclonal antibody
MFI	Mean fluorescence intensity
iNKT	Invariant natural killer T
PCR	Polymerase chain reaction
PBMC	Peripheral blood mononuclear cells
TCR	T cell receptor
XIAP	X-linked inhibitor of apoptosis
XLP	X-linked lymphoproliferative syndrome

Introduction

X-linked lymphoproliferative syndrome (XLP) is a rare inherited immunodeficiency estimated to affect approximately one in one million males, although it may be underdiagnosed [1]. XLP is characterized by extreme vulnerability to Epstein–Barr virus (EBV) infection, and the major clinical phenotypes of XLP include fulminant infectious mononucleosis (60%), lymphoproliferative disorder (30%), and dysgammaglobulinemia (30%) [2]. In addition, XLP is associated with a variety of additional clinical phenotypes such as vasculitis, aplastic anemia, and pulmonary lymphoid granulomatosis. Patients with XLP often develop more than one of these phenotypes. The gene responsible for XLP was identified as *SH2D1A*, located on Xq25 and encoding the SLAM-associated protein (SAP) [3–5]. However, gene analysis revealed *SH2D1A* mutations in only 50–60% of presumed XLP patients [6]. Importantly, a mutation in the gene that encodes the X-linked inhibitor of apoptosis (XIAP) called *XIAP* or *BIRC4* was identified as a second causative gene for XLP [7]. *XIAP* is located close to the *SH2D1A* gene on the X chromosome and consists of six coding exons [8–10]. XIAP produces an anti-apoptotic molecule that belongs to the inhibitor of apoptosis (IAP) family proteins. It contains three baculovirus IAP repeat (BIR) domains that, together with flanking residues, bind to caspases 3, 7, and 9, thereby inhibiting their proteolytic activity [11].

The clinical presentations of XIAP-deficient patients have been frequently reported [7,12,13]. More than 90% of patients with XIAP deficiency develop hemophagocytic lymphohistiocytosis (HLH) which is often recurrent. Therefore, it was recently suggested that the phenotype of XIAP deficiency fits better with the definition of familial HLH than with XLP disease [12]. However, familial HLH is characterized by defects in $CD8^+$ T and NK cell cytotoxicity responses, while these responses are normal in XIAP deficiency [7,12]. Other symptoms of XLP, such as splenomegaly, hypogammaglobulinema, and hemorrhagic colitis, have been reported in patients with XIAP deficiency, but lymphoma has never been noted [7,12–15].

We searched for patients with XIAP deficiency in Japan by detection of *XIAP* gene mutations and flow cytometric assessment of lymphoid XIAP expression. We previously reported the first case of XIAP deficiency in Japan [14]. Thereafter, we identified eight additional cases from five families with XIAP deficiency in our country. In this study, we describe the clinical and laboratory findings from nine patients from six unrelated families with XIAP deficiency, including previous cases, to help further the understanding of the pathogenetic features of this disease.

Materials and Methods

Patient and Family Member Samples

Patients without indentified *SH2D1A* mutations but with presumed XLP phenotypes were screened for *XIAP* mutations. Their family members were also screened for the same mutation. Upon identification of *XIAP* mutations, the patients were enrolled in this study. Patient 2.2 passed away before a genetic diagnosis of XIAP deficiency was made, but he was the maternal uncle of patient 2.1 and had presented with a XLP phenotype (Table I). In the end, nine patients from six different families were found to have XIAP deficiencies, three of whom had been reported previously [13,14]. Upon the approval of the Ethics Committee of the University of Toyama and after obtaining informed consent, 5–10 mL heparinized venous blood was collected from the patients, their mothers, and 25 age-matched healthy children (1–13 years of age). All of the samples were

X. Yang · H. Kanegane (✉) · N. Nishida · T. Miyawaki
Department of Pediatrics, Graduate School of Medicine, University of Toyama,
2630 Sugitani,
Toyama 930-0194, Japan
e-mail: kanegane@med.u-toyama.ac.jp

X. Yang · X.-D. Zhao
Division of Immunology,
Children's Hospital of Chongqing Medical University,
Chongqing, China

T. Imamura
Department of Pediatrics, Graduate School of Medical Sciences,
Kyoto Prefectural University of Medicine,
Kyoto, Japan

K. Hamamoto
Department of Pediatrics, Hiroshima Red Cross Hospital,
Hiroshima, Japan

R. Miyashita
Department of Pediatrics, Izumiotsu Municipal Hospital,
Izumiotsu, Japan

K. Imai · S. Nonoyama
Department of Pediatrics, National Defense Medical College,
Tokorozawa, Japan

K. Sanayama
Department of Pediatrics, Japanese Red Cross Narita Hospital,
Narita, Japan

A. Yamaide
Department of Allergy and Rheumatology,
Chiba Children's Hospital,
Chiba, Japan

F. Kato
Department of Pediatrics,
Tokyo Women's Medical University Medical Center East,
Tokyo, Japan

K. Nagai · E. Ishii
Department of Pediatrics,
Ehime University Graduate School of Medicine,
Toon, Japan

M. C. van Zelm
Department of Immunology, Erasmus MC,
Rotterdam, The Netherlands

S. Latour
INSERM U768, Hôpital Necker-Enfants Malades,
Paris, France

Published online: 08 January 2012

transferred to our laboratory at room temperature within 24 h for analysis.

Mutation Analysis of the *XIAP* Gene

DNA was extracted from peripheral blood using the QuickGene-Mini 80 nucleic acid extraction system (FUJIFILM Co., Tokyo, Japan). The coding regions and the exon–intron boundaries of the *XIAP* gene were amplified by polymerase chain reaction (PCR) using primers flanking each of the six exons by standard methods. PCR products were sequenced using the BigDye Terminator Cycle Sequencing Kit (Applied Biosystems, Foster City, CA, USA) with the same primers used for PCR amplification. Sequencing analysis was performed on an Applied Biosystems Prism 310 Capillary Sequencer (Applied Biosystems).

Flow Cytometric Analysis of XIAP Protein Expression in Lymphocytes

XIAP protein expression was studied by flow cytometric techniques as previously described [16,17]. Peripheral blood mononuclear cells (PBMC) from patients 1, 2.1, 3.1, 3.2, 4, 5, 6.1, 6.2, and 25 age-matched healthy children were prepared by density gradient centrifugation over Histopaque-1077 (Sigma-Aldrich, Inc., St. Louis, MO, USA). The cells were first fixed in 1% paraformaldehyde in PBS for 30 min at room temperature and then permeabilized in 0.5% saponin in washing buffer. The fixed and permeabilized cells were then incubated with an anti-XIAP monoclonal antibody (mAb) (clone 48 (BD Biosciences, Franklin Lakes, NJ, USA) or clone 2 F1 (Abcam, Cambridge, UK)) for 20 min on ice, washed, and then incubated with a FITC-labeled anti-mouse IgG1 antibody (SouthernBiotech, Birmingham, AL, USA) for 20 min on ice. The stained cells were analyzed on the FC500 flow cytometer (Beckman Coulter, Tokyo, Japan).

Western Blot Analysis of XIAP Protein Expression in Lymphocytes

PBMC from normal controls and patients 3.1, 5, and 6.2 were washed and pelleted. The cells were then lysed in 10 μL of lysing solution (1% Triton-X 100; 150 mmol/L NaCl; 10 mmol/L Tris–HCl, pH 7.6; 5 mmol/L EDTA-Na; 2 mmol/L phenylmethylsulfonyl fluoride) per 10^6 cells for 30 min on ice. The lysed cells were centrifuged for 10 min at 15,000*g* to remove nuclei, and the supernatants were diluted in the same volume of Laemmli's sample buffer. Samples were then electrophoresed in sodium dodecyl sulfate–polyarylamide 10% to 20% gradient gel and blotted on nitrocellulose filters. Blots were blocked in 5% skim milk in PBS for 1 h, treated with anti-XIAP mAb (clone 28 or clone 2F1) for 2 h, and then incubated with peroxidase-conjugated anti-mouse IgG antibody (Invitrogen, Grand Island, NY, USA) for 1 h. Immunoblots were developed by the ECL Western blotting detection system (GE Healthcare UK Ltd., Buckinghamshire, England).

Flow Cytometric Identification of Invariant Natural Killer T Cells

PBMC from eight patients (1, 2.1, 3.1, 3.2, 4, 5, 6.1, and 6.2) and 25 controls were incubated with fluorochrome-conjugated anti-CD3 (Dako Japan KK, Kyoto, Japan), anti-TCRVα24, and anti-TCRVβ11 mAbs (Beckman Coulter) to identify invariant natural killer T (iNKT) cells by flow cytometry. After the electronic gating of 100,000 $CD3^+$ T cells, iNKT cell populations were defined by the co-expression of TCRVα24 and TCRVβ11. The iNKT cell counts were evaluated at the diagnosis of XIAP deficiency.

Establishment of Alloantigen-Specific Cytotoxic T Lymphocyte Lines and Analysis of Cytotoxic T Lymphocyte-Mediated Cytotoxity

Alloantigen-specific $CD8^+$ cytotoxic T lymphocyte (CTL) lines were generated as described previously [18,19]. Briefly, PBMC were obtained from patients 1, 2.1, 3.1, and unrelated healthy individuals. These cells were co-cultured with a mitomycin C (MMC)-treated B lymphoblastoid cell line (LCL) established from an HLA-mismatched individual (KI-LCL). Using cell isolation immunomagnetic beads (MACS beads; Miltenyi Biotec, Auburn, CA, USA), $CD8^+$ T lymphocytes were isolated from PBMC that had been stimulated with KI-LCL for 6 days. $CD8^+$ T lymphocytes were cultured in RPMI 1640 medium supplemented with 10% human serum and 10 IU/mL interleukin-2 (Roche, Mannheim, Germany) and stimulated with MMC-treated KI-LCL three times at 1-week intervals. These lymphocytes were then used as $CD8^+$ alloantigen-specific CTL lines. The cytotoxic activity of CTLs was measured by a standard ^{51}Cr-release assay as described previously [20]. Briefly, alloantigen-specific CTLs were incubated with ^{51}Cr-labeled allogeneic KI-LCL or TA-LCL, which did not share HLA antigens with KI-LCL, for 5 h at effector/target cell ratios (E/T) of 2.5:1, 5:1, and 10:1. Target cells were also added to a well containing only medium and to a well containing 0.2% Triton X-100 to determine the spontaneous and maximum levels of ^{51}Cr release, respectively. After 5 h, 0.1 mL of supernatant was collected from each well. The percentage of specific ^{51}Cr release was calculated as follows: (cpm experimental release − cpm spontaneous release) / (cpm maximal release − cpm spontaneous release)×100, where cpm indicates counts per minute.

Table 1 Summary of our data

	Patient 1 [13]	Patient 2.1 [12]	Patient 2.2 [12]	Patient 3.1	Patient 3.2	Patient 4	Patient 5	Patient 6.1	Patient 6.2
Age at initial presentation	20 months	7 months	3 months	2 months	Asymptomatic	2 months	6 months	17 months	15 months
Current age	4 years	Deceased	Died of colitis	12 years	17 years	15 years	2 years	1 year	12 years
Family history	No	Yes	Yes	Yes	Yes	No	No	Yes	Yes
HLH	+	+	−	+	−	−	+	+	+
Recurrent HLH	+	+	−	+	−	−	+	−	+
Fever	+	+	+	+	−	−	+	+	+
Splenomegaly	+	+	ND	−	−	−	−	+	+
Cytopenia	+	+	ND	+	−	−	+	+	+
EBV	+	−	ND	+	−	−	−	+	+
Hypogammaglobulinemia	−	+	ND	−	−	+	−	−	−
Colitis	−	−	+	−	−	−	+	−	−
Treatment	PSL	PSL		PSL			PSL, Dex		
	CsA	CsA	ND	CsA	−	IVIG	CsA, IVIG	IVIG, Dex	PSL
	Dex	Dex					Infliximab		
Allogeneic HSCT	−	+	−	−	−	−	−	−	−
Mutation	R238X	R381X	ND	W217CfsX27	W217CfsX27	E349del	Del of exons 1-2	N341YfsX7	N341YfsX7
XIAP protein expression	±	−	ND	−	−	+	±	±	±

HLH hemophagocytic lymphohistiocytosis, *ND* no data, *EBV* Epstein–Barr virus, *PSL* prednisolone, *CsA* cyclosporin A, *Dex* dexamethasone, *IVIG* intravenous immunoglobulin, *HSCT* hematopoietic stem cell transplantation, + yes or positive, − no or negative, ± residual expression

Statistical Analysis

Student's *t*-test was used for statistics, with *P*-values <0.05 considered to be statistically significant.

Results

Clinical Manifestations of the Patients

Most of our patients presented with disease symptoms at very early ages; five patients presented in infancy and three patients presented in childhood (Table I). Three of the six families had family history records. Five of the nine patients had recurrent HLH, fever, splenomegaly, and cytopenia. EBV infection and hypogammaglobulinemia were also observed in multiple patients. Most patients with HLH were treated with corticosteroids with or without cyclosporin A to prevent an otherwise rapidly fatal disease course. Patients 2.2 and 5 presented with colitis, whereas patient 2.2 died; patient 5 improved with anti-TNF alpha mAb (infliximab®) treatment. Patient 2.1 underwent cord blood transplantation but died of complications. Patient 4 had a history of recurrent otitis media and pneumonia since 2 months of age, and he was found to have hypogammaglobulinemia. The patient was treated with intravenous immunoglobulin replacement therapy alone, and he is currently doing well. No patient developed lymphoma.

Detection of *XIAP* Mutations

We identified *XIAP* mutations in patients from all six unrelated families (Fig. 1) and analyzed all of the data using the US National Center for Biotechnology Information database (http://www.ncbi.nlm.nih.gov/SNP) to check for single-nucleotide polymorphism in the *XIAP* gene. As previously reported, patient 1 possessed a nonsense mutation, 712 C > T, resulting in an early stop codon R238X [14]. Patient 2.1 had a nonsense mutation in exon 5, 1141 C > T, resulting in R381X [13]. Patient 2.2 might have the same mutation as patient 2.1 because patient 2.2 was the maternal uncle of patient 2.1 [13]. Patients 3.1 and 3.2 were siblings and were found to have a one base pair deletion (650delG) in exon 1, resulting in a frameshift and premature stop codon (W217CfsX27). Patient 4 was found to have one amino acid deletion (1045_1047delGAG; E349del) in exon 3. Patient 5 has a large deletion, spanning exons 1 and 2. Patients 6.1 and 6.2 were brothers and had a two-nucleotide deletion (1021_1022delAA), which resulted in a frameshift and premature stop codon (N341YfsX7). All of the mothers of the patients from families 1–5 were heterozygote carriers of the mutations. Interestingly, we could not find any *XIAP* mutation in the mother of patients 6.1 and 6.2. We identified deleterious *XIAP* mutations in nine patients from six unrelated Japanese families that are likely to underlie their XLP phenotypes.

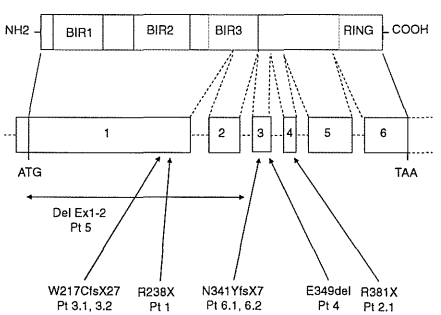

Fig. 1 *XIAP* gene mutations and their consequences for XIAP protein. *XIAP* comprises six exons and encodes the XIAP protein, which consists of 497 amino acids. XIAP contains three BIR domains and one RING domain. Mutations identified in our patients are indicated

XIAP Expression in Lymphocytes from the Patients and Carriers by Flow Cytometry

XIAP expression levels were analyzed in the lymphocytes of patients from all six families (Fig. 2). The lymphocytes of

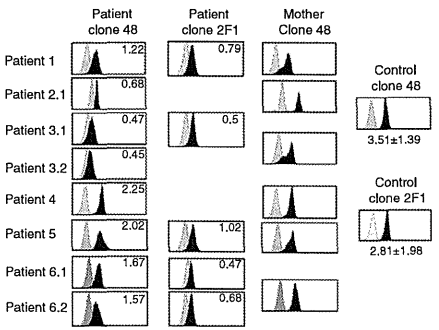

Fig. 2 XIAP protein expression in lymphocytes from the patients and their carriers. Flow cytometric detection of intracellular XIAP in lymphocytes from patients and their maternal carriers. The *gray* and *black areas* indicate the negative control and anti-XIAP staining, respectively. Anti-XIAP staining was performed using the clones 48 and 2 F1 antibodies where indicated. The *number in the box* indicates the log scale difference between the mean fluorescence intensity (ΔMFI) stained by the isotype antibody and that by the anti-XIAP antibodies. XIAP expression in 25 normal controls was also analyzed by the clone 48 and 2 F1 antibodies. The data of mean ± standard deviation of ΔMFI and each representative profile were shown

patients 1, 3.1, 5, 6.1, and 6.2 were examined by two different anti-XIAP mAbs. Using clone 48 antibody, patients 1, 2.1, 3.1, 3.2, 6.1, and 6.2 showed reduced XIAP expression, whereas XIAP was normally expressed in the lymphocytes of patients 4 and 5. In contrast to clone 48, clone 2F1 antibody showed reduced XIAP expression in patient 5. The effects of heterozygous *XIAP* mutations were studied in the lymphocytes of the patients' mothers by anti-XIAP mAb clone 48. The mothers of patients 1, 3.1, and 3.2 showed a bimodal pattern of XIAP protein (Fig. 2). The mothers of patients 2.1, 6.1, and 6.2 did not show a clear mosaic pattern, but all of these patients had reduced XIAP expression levels. Similarly to patients 4 and 5, the mothers of patients 4 and 5 demonstrated a normal XIAP expression pattern.

XIAP Expression in Lymphocytes from the Patients by Western Blot

Western blot analysis was used to evaluate the expression level of XIAP to determine the impact of patient *XIAP* mutations on protein expression and to compare this to the flow cytometric analysis. PBMCs from patients 3.1, 5.1, and 6.2 were available for Western blotting. All of these patients showed a reduction in XIAP protein expression (Fig. 3), fitting with the results obtained by flow cytometric analysis.

iNKT Cell Counts in the Patients

SAP-deficient patients had reduced numbers of NKT cells that expressed an invariantly rearranged T-cell receptor (TCR) consisting of TCRVα24 and TCRVβ11 chains [21,22]. The rare subset of iNKT cells was originally reported to be reduced in XIAP-deficient patients as well [7] but seemed to be present in normal numbers in a later study involving a larger patient cohort [23]. We analyzed the iNKT cell frequencies in 100,000 $CD3^+$ T cells in our XIAP-deficient patients and compared these with healthy controls (Fig. 4). The average frequency of iNKT cells within the $CD3^+$ T cell compartment of our XIAP patients was significantly reduced by twofold when compared with healthy

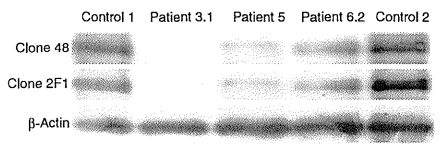

Fig. 3 XIAP expression in lymphocytes from the patients by Western blot. Analysis of XIAP expression in PBMC generated from patients with XIAP deficiency and normal controls using the antibody clone 48 (*upper panel*), the antibody clone 2 F1 (*middle panel*), and the β-actin antibody as an internal control (*lower panel*)

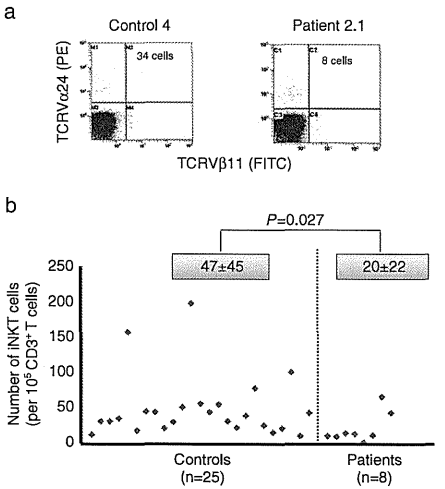

Fig. 4 iNKT cell counts in the patients and healthy controls. **a** Representative flow cytometric analysis of iNKT cells in $CD3^+$ lymphocytes from one XIAP-deficient patient and one healthy control. **b** Comparison of the number of iNKT cells in 100,000 $CD3^+$ lymphocytes between XIAP-deficient patients and control individuals. Statistical significance between patients and controls was determined with the Student's *t*-test (*p*-value=0.027)

controls (20 vs. 47 per 10^5 $CD3^+$ T cells). Therefore, we concluded that the number of iNKT cells was reduced in our patients with XIAP deficiency.

Functional Analysis of CTL Lines Established from the Patients

To test whether our XIAP-deficient patients have similar defects in $CD8^+$ T cell cytotoxicity as described in other subtypes of familial HLH [20,38], we generated $CD8^+$ alloantigen-specific CTL from patients 1, 2.1, 3.1, and three healthy controls (Fig. 5). The cytotoxic activity of the CTL of these patients was similar to that of the healthy controls, indicating that XIAP patients clearly differ from other familial HLH patients in this aspect of the disease.

Discussion

XIAP deficiency is a rare but severe and life-threatening inherited immune deficiency [12,13]. Early diagnosis and life-saving treatment such as hematopoietic stem cell transplantation is especially important. The causative gene for

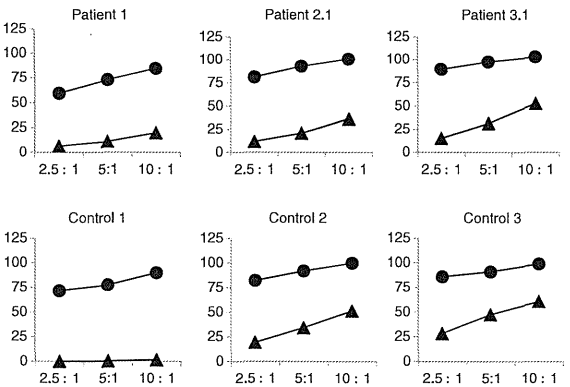

Fig. 5 Cytotoxicity of alloantigen-specific $CD8^+$ T cell lines. $CD8^+$ T cell lines were generated from PBMC of patients with XIAP deficiency and healthy controls by stimulation with allogeneic LCL (KI-LCL). Their cytotoxity was determined against allogeneic KI-LCL (*circles*) and against allogeneic TA-LCL (*triangles*), which does not share alloantigens with KI-LCL

XIAP deficiency was identified to be *XIAP/BIRC4*, and 25 mutations in the *XIAP* gene have been previously reported [7,12–14]. In the present study, we described four novel mutations (W217CfsX27, E349del, deletion of exons 1 and 2 and N341YfsX7) in the *XIAP* genes as well as previously described patients with R381X and R238X mutations [13,14]. The mother of patients 6.1 and 6.2 had no mutation in the *XIAP* gene. Because this is an X-linked inheritance, the failure to identify the same mutation in the mother suggests that the mother had a germline mosaicism for the mutation. Such mosaicism has not yet been described in XIAP deficiency, but it has been reported in Duchenne muscular dystrophy, X-linked severe combined immunodeficiency, X-linked agammaglobulinemia, and many other inherited diseases [24–26]. HLH is common in XIAP-deficient patients, and it is often recurrent [13,14]. In our study, six patients had HLH and five patients presented with recurrent HLH. Therefore, XIAP deficiency should be suspected in certain boys with HLH, especially in those with family history or recurrent HLH. The reason why XIAP deficiency increases susceptibility to HLH remains unclear. Murine studies have also failed to disclose a mechanism for the development of HLH [27]. Interestingly, Xiap-deficient mice possess normal lymphocyte apoptosis induced by a variety of means [28]. Three of our patients presented with EBV-associated HLH. EBV infection has been reported to be a trigger of the first HLH episode in patients with XIAP deficiency [13]. The excess of lymphocyte apoptosis in XIAP deficiency might account for the abnormal immune response to EBV [28]. Splenomegaly is not frequently observed in XLP type 1 or SAP deficiency but might be a common clinical feature in XIAP deficiency [12,13] as four (50%) of eight Japanese patients developed splenomegaly. Pachlopnik Schmid et al. [13] reported that recurrent splenomegaly occurring in the absence of systemic HLH was often associated with fever and cytopenia. XIAP-deficient patients are at risk for chronic colitis, which is possibly a more frequent cause of mortality than HLH [13]. Our study included two patients who developed colitis, and one of the patients died of colitis at 4 years of age. Although we did not have enough clinical information or samples from that patient because of his early death, his symptoms suggest that he had a XIAP deficiency complicated with colitis because he was the maternal uncle of patient 2.1. The other patient was 2 years old and also suffered from chronic hemorrhagic colitis.

In contrast to SAP deficiency, lymphoma has never been reported in XIAP deficiency, including our patients. Some studies indicate that the XIAP protein is a potential target for the treatment of cancer based on the anti-apoptotic function of XIAP [29]. Therefore, the absence of XIAP may protect patients from cancer, explaining why XIAP-deficient patients do not develop lymphoma. We generated a clinical summary to compare XIAP-deficient patients with the previous reports (Table II). Although our study included a relatively small number of patients, our results appear to be consistent with previous large studies [12,13] and confirm the clinical characteristics of XIAP deficiency.

Flow cytometry can be used for the rapid screening of several primary immunodeficiencies including XLP [30]. XIAP protein has been found to be expressed in various human tissues, including all hematopoietic cells [7,10]. Marsh et al. [16] described that XIAP was readily detectable in normal granulocytes, monocytes, and all lymphocyte subsets. Moreover, patients with *XIAP* mutations had decreased or absent expression of XIAP protein by flow cytometry [14,16]. We investigated XIAP expression in lymphocytes from eight patients by flow cytometry as previously described [16,17]. As demonstrated by Marsh et al. [16], clone 48 antibody provided brighter staining compared

Table II Comparison of patients with XIAP deficiency

	Marsh R et al. [12]	Pachlopnik Schmid J et al. [13]	Our study
Number of patients	10	30	9
HLH	9 (90%)	22/29 (76%)	6/9 (67%)
Recurrent HLH	6 (60%)	11/18 (61%))	5/6 (83%)
EBV-associated HLH	3 (30%)	16/19 (84%)	4/6 (67%)
Splenomegaly	9 (90%)	19/21 (90%)	4/8 (50%)
Hypogammaglobulinema	2 (20%)	8/24 (33%)	2/8 (25%)
Lymphoma	0	0	0
Colitis	0	5 (17%)	2 (22%)

to clone 2F1 antibody. In patients 5, 6.1, and 6.2, XIAP protein expression was normal when using clone 48 antibody but decreased when using clone 2F1 antibody. Western blot analysis showed XIAP expression in patients 3.1, ,5 and 6.2, and using clone 48 antibody, we found a discrepancy between flow cytometry and Western blot. Flow cytometric diagnosis may thus result in false positive results, and the gene sequencing of *XIAP* should be performed even when the patient shows normal XIAP expression levels.

All of the mothers examined in this study except for one were carriers of *XIAP* mutations. Analysis of XIAP expression in the mothers of patients 1, 3.1, and 3.2 revealed a bimodal expression pattern of XIAP in lymphocytes with cellular skewing towards expression of the wild-type XIAP allele as previously demonstrated [16]. However, the mother of patients 2.1, 6.1, and 6.2 demonstrated a normal expression pattern, possibly resulting from an extremely skewed pattern of X chromosome inactivation as shown in XIAP deficiency and other primary immunodeficiencies, and de novo mutations in *XIAP* are also observed [16,31]. The mother of patients 6.1 and 6.2 might have a germline mosaicism for the mutation, resulting in normal XIAP protein expression.

iNKT cells represent a specialized T lymphocyte subpopulation with unique features distinct from conventional T cells [32,33]. Human iNKT cells express an invariant TCR that recognizes self and microbacterial glycosphingolipid antigens presented by the major histocompatibility complex class I-like molecule CD1d [28]. The first series of XIAP-deficient patients showed decreased iNKT cell counts similar to SAP deficiency [7]. However, Xiap-deficient mice have normal numbers of iNKT cells and did not show an abnormal response to apoptotic stimuli [34]. Marsh et al. [23] reported a cohort of XIAP-deficient patients with normal numbers of iNKT cells, indicating that XIAP-deficient patients differ from SAP-deficient patients in this respect. In our cohort, we observed significantly decreased iNKT cell numbers in XIAP-deficient patients compared to healthy controls. However, we could not identify a correlation between the number of iNKT cells and the clinical disease features. Flow cytometric evaluation of iNKT cell counts can allow for the discrimination of XLP and other primary immunodeficiency diseases because patients may have normal XIAP protein expression in their lymphocytes.

CTLs kill their targets by one of two mechanisms: granule- or receptor-mediated apoptosis [35]. A recent study showed that the main pathway of cytotoxicity mediated by alloantigen-specific human $CD4^+$ and $CD8^+$ T cells is granule exocytosis and not the FAS/FAS ligand system [18]. Granzyme B is a major effector molecule of granule-mediated killing that rapidly induces cell death after entering the cytoplasm of the target cell [36]. The enzymatic activity of granzyme B is key to its ability to induce cell death. The executioner caspase-3 has been shown to be proteolytically processed and activated by granzyme B [37]. Although XIAP possesses an inhibitory effect for caspases, it is important to study the cytotoxic activities of CTLs in XIAP deficiency. Furthermore, many studies have indicated that some subtypes of patients with familial HLH show a deficiency in their cytotoxic activities [20,38]. To further investigate the function of antigen-specific CTLs, we studied $CD8^+$ alloantigen-specific CTL analysis among three XIAP-deficient patients. XIAP-deficient patients showed a normal level of cytotoxic activity, suggesting that XIAP might not play an important role in the cytotoxic responses of $CD8^+$ T cells as was previously suggested based on the normal NK cell-mediated cytotoxicity found in XIAP-deficient patients [7,12].

In this study, we have described nine Japanese patients with XIAP deficiency with clinical characteristics similar to those of patients in Europe and USA [12,13].

Acknowledgments This study was supported by Grant-in-Aids for Scientific Research from the Ministry of Education, Culture, Sports, Science and Technology (H. Kanegane and T. Miyawaki) and grants from the Ministry of Health, Labour, Welfare of Japan (T. Miyawaki), the XLP Reserch Trust (S. Latour) and Agence Nationale pour la Recherche (ANR-08-MIEN-012-01) and an Erasmus MC Fellowship (M.C. van Zelm). We thank Ms. Chikako Sakai and Mr. Hitoshi Moriuchi for their excellent technical assistance. We are also grateful for the support, cooperation, and trust of the patients and their families.

References

1. Sumegi J, Huang D, Lanyi A, Davis JD, Seemayer TA, Maeda A, et al. Correlation of mutations of the SH2D1A gene and Epstein–Barr virus infection with clinical phenotype and outcome in X-linked lymphoproliferative disease. Blood. 2000;96:3118–25.
2. Seemayer TA, Gross TG, Egeler RM, Pirruccello SJ, Davis JR, Kelly CM, et al. X-linked lymphoproliferative disease: twenty-five years after the discovery. Pediatr Res. 1995;38:471–8.
3. Sayos J, Wu C, Morra M, Wang N, Zhang X, Allen D, et al. The X-linked lymphoproliferative-disease gene product SAP regulates signals induced through the co-receptor SLAM. Nature. 1998;395:462–9.
4. Coffey AJ, Brooksbank RA, Brandau O, Oohashi T, Howell GR, Bye JM, et al. Host response to EBV infection in X-linked lymphoproliferative disease results from mutations in an SH2-domain encoding gene. Nat Genet. 1998;20:129–35.
5. Nichols KE, Harkin DP, Levitz S, Krainer M, Kolquist KA, Genovese C, et al. Inactivating mutations in an SH2 domain-encoding gene in X-linked lymphoproliferative syndrome. Proc Natl Acad Sci USA. 1998;95:13765–70.
6. Gilmour KC, Cranston T, Jones A, Davies EG, Goldblatt D, Thrasher A, et al. Diagnosis of X-linked lymphoproliferative disease by analysis of SLAM-associated protein expression. Eur J Immunol. 2000;30:1691–7.
7. Rigaud S, Fondanèche MC, Lambert N, Pasquier B, Mateo V, Soulas P, et al. XIAP deficiency in humans causes an X-linked lymphoproliferative syndrome. Nature. 2006;444:110–4.
8. Uren AG, Pakusch M, Hawkins CJ, Puls KL, Vaux DL. Cloning and expression of apoptosis inhibitory protein homologs that function to inhibit apoptosis and/or bind tumor necrosis factor receptor-associated factors. Proc Natl Acad Sci USA. 1996;93:4974–8.
9. Liston P, Roy N, Tamai K, Lefebvre C, Baird S, Cherton-Horvat G, et al. Suppression of apoptosis in mammalian cells by NAIP and a related family of IAP genes. Nature. 1996;379:349–53.
10. Duckett CS, Nava VE, Gedrich RW, Clem RJ, van Dongen JL, Gilfillan MC, et al. A conserved family of cellular genes related to the baculovirus iap gene and encoding apoptosis inhibitors. EMBO J. 1996;15:2685–94.
11. Galbán S, Duckett CS. XIAP as a ubiquitin ligase in cellular signaling. Cell Death Differ. 2010;17:54–60.
12. Marsh RA, Madden L, Kitchen BJ, Mody R, McClimon B, Jordan MB, et al. XIAP deficiency: a unique primary immunodeficiency best classified as X-linked familial hemophagocytic lymphohistiocytosis and not as X-linked lymphoproliferative disease. Blood. 2010;7:1079–82.
13. Pachlopnik Schmid J, Canioni D, Moshous D, Touzot F, Mahlaoui N, Hauck F, et al. Clinical similarities and differences of patients with X-linked lymphoproliferative syndrome type 1 (XLP-1/SAP-deficiency) versus type 2 (XLP-2/XIAP-deficiency). Blood. 2011;117:1522–9.
14. Zhao M, Kanegane H, Ouchi K, Imamura T, Latour S, Miyawaki T. A novel XIAP mutation in a Japanese boy with recurrent pancytopenia and splenomegaly. Haematologica. 2010;95:688–9.
15. Filipovich AH, Zhang K, Snow AL, Marsh RA. X-linked lymphoproliferative syndromes: brothers or distant cousins? Blood. 2010;116:3398–408.
16. Marsh RA, Villanueva J, Zhang K, Snow AL, Su HC, Madden L, et al. A rapid flow cytometric screening test for X-linked lymphoproliferative disease due to XIAP deficiency. Cytometry B Clin Cytom. 2009;76:334–44.
17. Marsh RA, Bleesing JJ, Filipovich AH. Using flow cytometry to screen patients for X-linked lymphoproliferative disease due to SAP deficiency and XIAP deficiency. J Immunol Methods. 2010;362:1–9.
18. Yasukawa M, Ohminami H, Arai J, Kasahara Y, Ishida Y, Fujita S. Granule exocytosis, and not the fas/fas ligand system, is the main pathway of cytotoxity mediated by alloantigen-specific CD4(+) as well as CD8(+) cytotoxic T lymphocytes in humans. Blood. 2000;95:2352–5.
19. Yanai F, Ishii E, Kojima K, Hasegawa A, Azuma T, Hirose S, et al. Essential roles of perforin in antigen-specific cytotoxity mediated by human CD4+ T lymphocytes: analysis using the combination of hereditary perforin-deficient effector cells and Fas-deficient target cells. J Immunol. 2003;170:2205–13.
20. Ishii E, Ueda I, Shirakawa R, Yamamoto K, Horiuchi H, Ohga S, et al. Genetic subtypes of familial hemophagocytic lymphohistiocytosis: correlations with clinical features and cytotoxic T lymphocyte/natural killer cell functions. Blood. 2005;105:3442–8.
21. Nichols KE, Hom J, Gong SY, Ganguly A, Ma CS, Cannons JL, et al. Regulation of NKT cell development by SAP, the protein defective in XLP. Nat Med. 2005;11:340–5.
22. Pasquier B, Yin L, Fondanéche MC, Relouzat F, Bloch-Queyrat C, Lambert N, et al. Defective NKT cell development in mice and humans lacking the adapter SAP, the X-linked lymphoproliferative syndrome gene product. J Exp Med. 2005;201:695–701.
23. Marsh RA, Villanueva J, Kim MO, Zhang K, Marmer D, Risma KA, et al. Patients with X-linked lymphoproliferative disease due to *BIRC4* mutation have normal invariant natural killer T-cell populations. Clin Immunol. 2009;132:116–23.
24. Puck JM, Pepper AE, Bedard PM, Laframboise R. Female germ line mosaicism as the origin of a unique IL-2 receptor gamma-chain mutation causing X-linked severe combined immunodeficienc. J Clin Invest. 1995;95:895–9.
25. O'Marcaigh A, Puck JM, Pepper AE, Santes KD, Cowan MJ. Maternal mosaicism for a novel interleukin-2 receptor gamma-chain mutation causing X-linked severe combined immunodeficiency in a Navajo kindred. J Clin Immunol. 1997;17:29–33.
26. Sakamoto M, Kanegane H, Fujii H, Tsukada S, Miyawaki T, Shinomiya N. Maternal germinal mosaicism of X-linked agammaglobulinemia. Am J Med Genet. 2001;99:234–7.
27. Harlin H, Reffey SB, Duckett CS, Lindsten T, Thompson CB. Characterization of XIAP-deficient mice. Mol Cell Biol. 2001;21:3604–8.
28. Latour S. Natural killer T cells and X-linked lymphoproliferative syndrome. Curr Opin Allergy Clin Immunol. 2007;7:510–4.
29. Schimmer AD, Dalili S, Batey RA, Riedl SJ. Targeting XIAP for the treatment of malignancy. Cell Death Differ. 2006;13:179–88.
30. Oliveira JB, Notarangelo LD, Fleisher TA. Applications of flow cytometry for the study of primary immune deficiencies. Curr Opin Allergy Clin Immunol. 2008;8:499–509.
31. Kanegane H, Futatani T, Wang Y, Nomura K, Shinozaki K, Matsukura H, et al. Clinical and mutational characteristics of X-linked agammaglobulinemia and its carrier identified by flow cytometric assessment combined with genetic analysis. J Allergy Clin Immunol. 2001;108:1012–20.
32. Godfrey DI, Berzins SP. Control points in NKT-cell development. Nat Rev Immunol. 2007;7:505–18.
33. Bendelac A, Savage PB, Teyton L. The biology of NKT cells. Annu Rev Immunol. 2007;25:297–336.
34. Bauler LD, Duckett CS, O'Riordan MX. XIAP regulates cytosol-specific immunity to *Listeria* infection. PLoS Pathog. 2008;4:e1000142.
35. Hersperger AR, Makedonas G, Betts MR. Flow cytometric detection of perforin upregulation in human CD8 T cells. Cytometry A. 2008;73:1050–7.
36. Motyka B, Korbutt G, Pinkoski MJ, Heibein JA, Caputo A, Hobman M, et al. Mannose 6-phosphate/insulin-like growth factor II receptor is a death receptor for granzyme B during cytotoxic T cell-induced apoptosis. Cell. 2000;103:491–500.
37. Martin SJ, Amarante-Mendes GP, Shi L, Chuang TH, Casiano CA, O'Brien GA, et al. The cytotoxic cell protease granzyme B initiates apoptosis in a cell-free system by proteolytic processing and activation of the ICE/CED-3 family protease, CPP32, via a novel two-step mechanism. EMBO J. 1996;15:2407–16.
38. zur Stadt U, Rohr J, Seifert W, Koch F, Grieve S, Pagel J, et al. Familial hemophagocytic lymphohistiocytosis type 5 (FHL-5) is caused by mutations in Munc18-2 and impaired binding to syntaxin 11. Am J Hum Genet. 2009;85:482–92.

J Clin Immunol

Springer

Bone Marrow Transplantation (2012) 47, 1126–1127

www.nature.com/bmt

LETTER TO THE EDITOR

Allo-SCT in a patient with CRMCC with aplastic anemia using a reduced intensity conditioning regimen

Bone Marrow Transplantation (2012) **47,** 1126–1127; doi:10.1038/bmt.2011.221; published online 14 November 2011

Cerebroretinal microangiopathy with calcifications and cysts (CRMCC; Revesz syndrome)[1–3] is a rare congenital systemic disorder that was first described by Revesz *et al.* in 1992.[1] It is characterized by intrauterine growth retardation, bilateral exudative retinopathy, intracranial calcification and cysts, leukoencephalopathy, sparse hair, nail dystrophy, and skeletal defects. Approximately one-third of cases are complicated by the development of hematological disorders; in particular, aplastic anemia similar to that observed in dyskeratosis congenita (DKC).[4–6] CRMCC with aplastic anemia and DKC both belong to the congenital BM-failure disease spectrum and additional similarities between these two diseases have been reported, including shortened telomere length and mutations of the *TINF2*, which encodes TIN2 (a regulator of telomere length in human cells).[4,7,8] Similar to DKC, aplastic anemia associated with CRMCC can be cured only by hematopoietic SCT (HSCT); however, to date HSCT has not been widely used in this patient population.[4,7,8] Herein, we report a case of CRMCC associated with a *TINF2* mutation, which was successfully treated with HSCT using a fludarabine-based reduced-intensity conditioning (RIC) regimen.

The patient was a Japanese boy who was born at 38 weeks gestation to non-consanguineous parents and had a birth weight of 2.57 kg (−0.8 s.d.). There was no family history of ocular or neurological disease. The neonatal period was uneventful and his development was considered normal until 1 year of age. Nail dystrophy was noted, but he displayed no signs of leukoplakia or skin disease. At the age of 15 months, his mother first noticed a right divergent squint. Subsequent ophthalmological investigation revealed bilateral exudative retinopathy and retinal detachment, consistent with bilateral Coats' disease (Figure 1a). Truncal ataxia with normal deep-tendon- and superficial-skin-reflexes was noted on neurological examination. At the age of 17 months, brain computed tomography (CT) scanning demonstrated extensive intracranial calcifications. T2-weighted magnetic resonance imaging of the brain revealed spotty high signals within the white matter of the brainstem, the deep gray nuclei, and the right frontal and parietal lobes (Figure 1b and c). A cystic mass adjacent to the thalamus was also observed. Macrocytic anemia and severe thrombocytopenia were also detected (red blood cell, 301×10^4 per μL; hemoglobin level, 9.8 g/dl; mean corpuscular volume (MCV), 98.3 fl; reticulocyte count: 37 000 per μL; platelet count: 8000 per μL). No leukopenia or neutropenia was observed (white blood cell, 5100 per μL with an ANC of 1479 per μL). BM aspiration revealed hypoplastic BM (nucleated cell count: 41 500 per μL and megakaryocytes 0 per μL, with no dysplastic features). G-banding analysis of the BM at 18 months revealed the karyotype 48, XY, +2 mar (1/16)/46, XY (15/16). A chromosomal breakage study showed no excess of mitomycin C-induced breaks, which indicated that Fanconi's anemia was not present (data not shown). Flow-FISH analysis in PBLs demonstrated shortened telomere length and DNA sequencing identified a heterozygous missense mutation (845 G>A, R282H) of the *TINF2* gene (Figure 1d). *TINF2* encodes TIN2, one of the key components of shelterin, a protein complex that stabilises telomeres.[7] Mutated amino acids were tightly clustered in the position between 280 and 290 in classic DKC or CRMCC patients.[7,8]

On the basis of these findings, a diagnosis of CRMCC was made. At the age of 17 months, the exudative retinopathy was successfully treated with laser coagulation, pars plana vitrectomy and the intra-vitreal administration of vascular endothelial growth factor inhibitors. However, at the age of 22 months, the bicytopenia became more severe and treatment with prednisolone (1 mg/kg/day) and danazol (5 mg/kg/day) was initiated. In response, the anemia improved slightly, but there was no effect on the thrombocytopenia, although bleeding tendency was not evident. Thus, we decided to perform allogeneic HSCT with an HLA-matched, related, healthy female donor. The conditioning regimen was as follows: 25 mg/m^2 fludarabine daily on days −5 to −2; 25 mg/kg CY daily on days −5 to −2 and 1.25 mg/kg anti-thymocyte globulin (Thymoglobulin) daily on days −5 to −2. Total nucleated cell and CD34+ doses were 2.48×10^8 and 2.08×10^6 per kg recipient body weight, respectively. GVHD prophylaxis consisted of CsA and short term MTX. Desired neutrophil counts (>500 per μL) were obtained by day 12, reticulocyte counts (>1.0%) by day 20, and platelet counts ($>5.0 \times 10^4$ per μL) by day 48. Genotyping using XY-FISH analysis of a BM sample taken at day 48 revealed that 98.4% of total nucleated cells were of donor origin. The post-transplant course was uneventful with grade 1 oral mucositis being the only complication. Neither acute nor chronic GVHD was evident. The patient is currently 20 months post transplant without any immunosuppressants and transplantation-related complication.

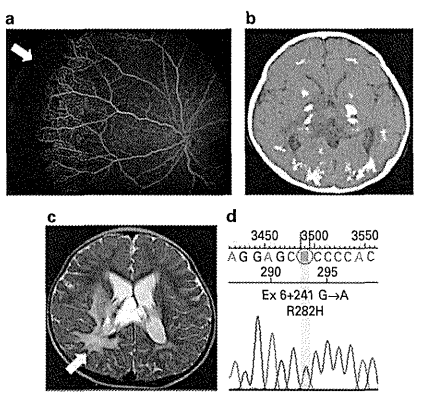

Figure 1. (**a**) Fluorescein angiogram. The arrow indicates an avascular peripheral zone in the left eye, which suggests retinal detachment. (**b**) CT of the brain. CT of the brain revealed extensive intracranial calcification, which is characteristic to CRMCC. (**c**) T2-weighted magnetic resonance imaging of the brain. The arrow indicates high signals within the white matter of the right parietal lobe, suggesting the presence of leukoencephalopathy. (**d**) Sequence tracing showing a TINF2 mutation in PBLs of the patient. Sequence tracing showing a heterozygous G to A mutation (Ex 6 +241 G→A, R282H) in *TINF2*.

In surveying the literature, we found that in CRMCC,[1–9] at least one of the DKC triad of dystrophic nail, abnormal skin findings and leukoplakia was noted significantly more frequently in positive vs negative hematological disorder (one of DKC triad, 10/17 vs 5/23, $P<0.01$; dystrophic nail, 9/16 vs 4/23, $P<0.01$; leukoplakia, 3/5 vs 0/9, $P<0.05$). We found two previous reports of CRMCC patients with an identical mutation in *TINF2* to that in our patient.[7,8]

Kajtar *et al.*[4] described a 2-year-old girl with CRMCC successfully treated with allogeneic BMT from an HLA-identical brother. The post-transplantation course in this patient was uneventful with only mild GVHD. Savage *et al.*[7] described a case of CRMCC who died after BMT; however, detailed information on the conditioning regimen was not available. Walne *et al.*[8] also described four cases of CRMCC with a *TINF2* mutation, of which one received BMT, but details on the conditioning regimen and transplantation courses were not reported. In DKC, circulating lymphocytes and fibroblasts exhibit an increased *in vitro* sensitivity to radiation and alkylating agents.[10] Therefore, this suggested that HSCT using myeloablative conditioning regimens in DKC patients would be associated with high regimen-related toxicity.[10] For this reason, RIC regimens are strongly recommended in HSCT for DKC patients.[11] Herein, we used a RIC regimen for our patient, which was safe and had minimal toxicity. Our experience suggests that HSCT with a RIC regimen should be considered for treatment of CRMCC patients with hematological disorders.

CONFLICT OF INTEREST

The authors declare no conflict of interest.

ACKNOWLEDGEMENTS

The authors thank Dr Shinsaku Imashuku for his critical reading of the manuscript and Ms Yasuko Hashimoto for her secretarial assistance.

D Asai[1], S Osone[2], T Imamura[1], H Sakaguchi[3], N Nishio[3], H Kuroda[2], S Kojima[3] and H Hosoi[1]
[1]*Department of Pediatrics, Kyoto Prefectural University of Medicine, Graduate School of Medical Science, Kyoto, Japan;*
[2]*Division of Pediatrics, Kyoto City Hospital, Kyoto, Japan;*
[3]*Department of Pediatrics, Nagoya University Graduate School of Medicine, Nagoya, Japan*
E-mail: imamura@koto.kpu-m.ac.jp

REFERENCES

1 Revesz T, Fletcher S, al-Gazali LI, DeBuse P. Bilateral retinopathy, aplastic anaemia, and central nervous system abnormalities: A new syndrome? *J Med Genet* 1992; **29**: 673–675.
2 Goutieres F, Dollfus H, Becquet F, Duffer JL. Extensive brain calcification in two children with bilateral Coats disease. *Neuropediatrics* 1999; **30**: 19–21.
3 Briggs TA, Abdel-Salam GMH, Balicki M. Cerebroretinal microangiopathy with calcifications and cysts (CRMCC). *Am J Med Genet A* 2008; **146A**: 182–190.
4 Kajtar P, Mehes K. Bilateral coats retinopathy associated with aplastic anaemia and mild dyskeratotic signs. *Am J Med Genet* 1994; **49**: 374–377.
5 Duprey PA, Steger JW. An unusual case of dyskeratosis congenita with intracranial calcifications. *J Am Acad Dermatol* 1988; **19**: 760–762.
6 Gayatri NA, Hughes MI, Lloyd IC, Wynn RF. Association of the congenital bone marrow failure syndromes with retinopathy, intracerebral calcification and progressive neurological impairment. *Eur J Paediatr Neurol* 2002; **6**: 125–128.
7 Savage SA, Giri N, Baerlocher GM, Orr N, Lansdorp PM, Alter BP. *TINF2*, a component of sheltrin telomere protection complex, is mutated in dyskeratosis congenita. *Am J Hum Genet* 2008; **82**: 501–509.
8 Walne AJ, Vulliamy T, Beswick R, Kirwan M, Dokal I. *TINF2* mutations result in very short telomeres: analysis of a large cohort of patients with dyskeratosis congenita and related bone marrow failure syndromes. *Blood* 2008; **112**: 3594–3600.
9 Crow YJ, McMenamin J, Haenggeli CA, Hadley DM, Tirupathi S, Treacy EP *et al.* Coat's Plus:A progressive familial syndrome of bilateral Coat's disease, characteristic cerebral calcification, leukoencephalopathy, slow pre- and post-natal linear growth and defects of bone marrow and integument. *Neuropediatrics* 2004; **35**: 10–19.
10 M'kacher R, Laithier V, Valent A, Delhommeau F, Violot D, Deutsch E *et al.* Sensitivity to radiation and alkylation agent of peripheral lymphocytes and fibroblasts in a Hoyeraal-Hreidarsson syndrome patient. *Pediatr Hematol Oncol* 2003; **20**: 651–656.
11 Dietz AC, Orchard PJ, Baker KS, Giller RH, Savage SA, Alter BP *et al.* Disease-specific hematopoietic cell transplantation: nonmyeloablative conditioning regimen for dyskeratosis congenita. *Bone Marrow Transplant* 2011; **46**: 98–104.

Allo-SCT in a patient with CRMCC with aplastic anemi... http://www.nature.com/bmt/journal/v47/n8/pdf/bmt2...

INTERNAL MEDICINE

□ CASE REPORT □

A Case of Congenital Dyserythropoietic Anemia Type 1 in a Japanese Adult with a *CDAN1* Gene Mutation and an Inappropriately Low Serum Hepcidin-25 Level

Hiroshi Kawabata[1], Sayoko Doisaki[2], Akio Okamoto[3], Tatsuki Uchiyama[1], Soichiro Sakamoto[1], Asahito Hama[2], Kiminori Hosoda[4], Junji Fujikura[5], Hitoshi Kanno[6], Hisaichi Fujii[6], Naohisa Tomosugi[7], Kazuwa Nakao[5], Seiji Kojima[2] and Akifumi Takaori-Kondo[1]

Abstract

We describe the first case of genetically diagnosed congenital dyserythropoietic anemia (CDA) type 1 in a Japanese man. The patient had hemolytic anemia since he was a child, and he developed diabetes, hypogonadism, and liver dysfunction in his thirties, presumably from systemic iron overload. When he was 48 years old a diagnosis was finally made by genetic analysis that revealed a homozygous mutation of *CDAN1* gene (Pro1129Leu). His serum hepcidin-25 level was inappropriately low. We conclude that physicians should be aware of the possibility of CDA in a patient with anemia and systemic iron overload at any age.

Key words: congenital dyserythropoietic anemia, iron metabolism, hemochromatosis, hepcidin, growth differentiation factor-15

(Intern Med 51: 917-920, 2012)
(DOI: 10.2169/internalmedicine.51.6978)

Introduction

Congenital dyserythropoietic anemia (CDA) is a rare congenital erythropoietic disorder with characteristic morphological abnormalities of the bone marrow cells, ineffective erythropoiesis and systemic iron overload (1). Three types of CDA are known: types 1, 2 and 3. The genes responsible for types 1 and 2 have recently been identified as *CDAN1* and *SEC23B*, respectively (2, 3). Both CDA types 1 and 2 are inherited recessively. The incidence of CDA is very rare, and in a recent pan-European survey, only 124 CDA type 1 cases were recorded (4). To date, several Japanese CDA type 1 cases have also been reported (5-7), but none of them has been genetically proven. Here, we describe in a Japanese adult a case of CDA type 1 with systemic iron overload that was genetically diagnosed in his late forties.

Case Report

A Japanese man was referred to the Kyoto University Hospital for hyperglycemia when he was 38 years old. He had had hemolytic anemia since he was a child, but its etiology had not been determined. He had undergone splenectomy when he was 36 years old, which ameliorated his anemia to some extent. At his first visit to our hospital, his white blood cell count was 6,400/μL; red blood cell count, 1.93×10^6/μL; hemoglobin (Hb) level, 7.5 g/dL; hematocrit level, 21.0%; mean corpuscular volume, 108.8 fL; platelet count, 365×10^3/μL; and reticulocyte count, 53×10^3/μL (Table 1). He had hepatic dysfunction, with a slightly elevated serum alanine aminotransferase level (68 IU/L), hyperglycemia (blood sugar level of 146 mg/dL and HbA1c level of 6.9%) with very low insulin secretion (serum c-peptide level, <0.1 ng/mL), and hypogonadism with a serum testosterone level lower than 0.2 ng/mL, i.e., very low (reference range, 2.7-10.7 ng/mL). His blood test results also suggested iron overload (transferrin saturation of 95.3% and serum ferritin level of 4,058 ng/mL), and the liver biopsy results revealed marked accumulation of iron in the parenchymal cells. Thus, hemochromatosis, along with liver dysfunction, diabetes and hypogonadism, was diagnosed. Insulin therapy was then started. Occasional phlebotomy was also started to remove excess iron and to gradually decrease his serum ferritin and alanine aminotransferase levels to within the reference ranges (Table 1). When he was 46 years old, a series of intensive diagnostic examinations were started. The findings of the biochemical analyses for erythrocyte membrane disorders or unstable hemoglobinopathies were all negative. The bone marrow examination revealed marked erythroid hyperplasia (the myeloid to erythroid ratio of 0.34) and remarkable dysplastic features in the erythroid cells, with megaloblastoid changes and multinuclear cells (Fig. 1A-E). However, no significant dysplasia was observed in the granulocytic or megakaryocytic series (Fig. 1A, B), and no ring sideroblasts were observed in the iron staining. When he was 48 years old, we obtained his written informed consent and approval by the ethics committee of Kyoto University to perform a genetic analysis for indicators of hereditary iron disorders in his peripheral blood cells. The results of the genetic analyses for pyruvate kinase deficiency and thalassemia syndromes were all negative. There were no mutations in the exons and the exon-intron borders of hereditary hemochromatosis genes including *HFE*, *TFR2*, *HJV*, *HAMP*, and *SLC40A1*. However, a homozygous mutation in *CDAN1 ex26 c.3503 C>T* (Pro1129Leu) was detected, consistent with CDA type 1 (Fig. 2). When we reviewed his bone marrow specimen, internuclear bridges that connected two separate erythroblasts were occasionally observed (7 bridges in 500 erythroblasts, Fig. 1F-J). His serum hepcidin-25 level was 0.8 ng/mL [reference range, 2.3-37 ng/mL; analyzed with a quantitative liquid chromatography coupled with tandem mass spectrometry method (8)]. The growth differentiation factor-15 (GDF15) level was 8,469 pg/mL (reference range, 215-835 pg/mL; analyzed with a commercial ELISA kit from R&D, Minneapolis, MN). The patient had two siblings, a brother and a sister; both were in good health. There was no significant family history except that his mother had anemia of undetermined etiology, and his paternal grandfather had diabetes. He declined genetic analysis of his family for the *CDAN1* gene.

Table 1. **Laboratory Data**

Features	Laboratory data at the first visit (38 years old)	Laboratory data at the time of diagnosis (48 years old)
White blood cells (per μL)	6.4×10^3	5.3×10^3
Red blood cells (per μL)	1.93×10^6	2.41×10^6
Hemoglobin (g/dL)	7.5	8.5
Hematocrit (%)	21.0	24.1
Reticulocytes (per μL)	53×10^3	—
Platelet counts (per μL)	365×10^3	312×10^3
Total bilirubin (mg/dL)	1.5	1.6
Direct bilirubin (mg/dL)	0.7	0.1
Haptoglobin (mg/dL)	<7.9	—
AST (IU/L)	49	26
ALT (IU/L)	68	16
LDH (IU/L)	302	277
Ferritin (ng/mL)	4058	186

— indicates that the tests were not performed. Abbreviations; AST, aspartate aminotransferase (reference range, 13-29 IU/L); ALT, alanine aminotransferase (reference range, 8-28 IU/L); LDH, lactate dehydrogenase (reference range, 129-241 IU/L).

Discussion

We encountered an adult patient with hemolytic anemia with various symptoms caused by systemic iron overload, who turned out to have a genetic mutation consistent with CDA type 1. To our knowledge, this is the first documented case of CDA type 1 in a Japanese with *CDAN1* gene mutation. Dgany et al. identified the same *CDAN1* gene mutation as the current case in a French Polynesian family (2). *CDAN1* is located on chromosome 15q15.1-15q15.3, and it codes for a nuclear protein, codanin-1, the human homolog of discs lost (dlt) which is required for cell survival and cell cycle progression in *Drosophila* (9). The diagnosis of CDA type 1 has usually been made from clinical features together with characteristic morphological features of the bone marrow cells such as binucleated erythroblasts, and internuclear bridges between the erythroid cells. As codanin-1 is essential for proper cellular trafficking of the heterochromatin

[1]Department of Hematology and Oncology, Graduate School of Medicine, Kyoto University, Japan, [2]Department of Pediatrics, Nagoya University Graduate School of Medicine, Japan, [3]Nantan General Hospital, Japan, [4]Faculty of Human Health Science, Kyoto University Graduate School of Medicine, Japan, [5]Department of Medicine and Clinical Science, Kyoto University Graduate School of Medicine, Japan, [6]Department of Transfusion Medicine and Cell Processing, Tokyo Women's Medical University, Japan and [7]Division of Advanced Medicine, Medical Research Institute, Kanazawa Medical University, Japan
Received for publication November 21, 2011; Accepted for publication January 5, 2012
Correspondence to Dr. Hiroshi Kawabata, hkawabat@kuhp.kyoto-u.ac.jp

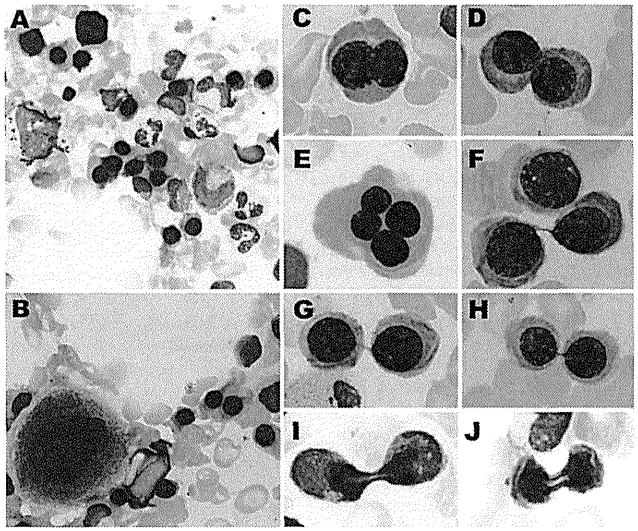

Figure 1. **Bone marrow cell morphology (May-Grünwald-Giemsa staining, original magnification ×1,000; C-J, images were further magnified by photographic enlargement). A and B: Erythroid hyperplasia. No significant dysplasia was observed in the granulocytic or megakaryocytic series. C and D: Binucleated erythroblasts. These cells were found in approximately 12% of the erythroblasts. E: A few tetranucleated erythroblasts were found. F-J: Internuclear bridges between the erythroblasts were found after careful inspection.**

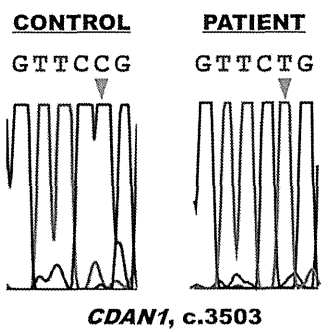

Figure 2. **The homozygous mutation in *CDAN1* (*ex26 c.3503 C>T*, Pro1129Leu) detected in the patient.**

protein HP1-α (10), defects of this protein may result in such morphological abnormalities. In the current case, the bone marrow examination results showed numerous binucleated erythroblasts, but the internuclear bridges, which are much more specific features of this disorder, were observed in less than 3% of the erythroblasts and were overlooked in the first inspection (Fig. 1). Therefore, making a definitive diagnosis of CDA from bone marrow cell morphology alone can sometimes be difficult.

CDA types 1 and 2 are known to be accompanied by iron overload. Similar to hereditary hemochromatosis, inappropriately low production of hepcidin, the central regulator of systemic iron homeostasis, has been proposed as the etiology of iron overload in CDA (11). As the main function of hepcidin is to downregulate the expression of ferroportin, the only known cellular iron exporter of mammals, downregulation of hepcidin results in an increase in ferroportin expression, thereby increasing iron absorption from the intestine and causing systemic iron overload. A previous report demonstrated marked increases of GDF15 in the serum of CDA type 1 patients (12). GDF15, a humoral factor belonging to the transforming growth factor-β superfamily, has been shown to suppress hepatic production of hepcidin (13). Consistent with the previous reports, systemic iron overload was induced in the current case without repeated red cell transfusions, the serum GDF15 level was remarkably elevated, and the serum hepcidin-25 level was inappropriately low. Thus, we postulate that serum hepcidin-25 and GDF15 are useful markers for CDA.

CDA is generally regarded as a pediatric disease because the initial symptoms, such as anemia, jaundice, and splenomegaly, usually appear in the first decade. However, the current case was diagnosed when the patient was in his late forties, and in the pan-European survey, CDA was diagnosed in a substantial proportion of patients who were middle-aged or older (4). Early diagnosis of CDA is important because iron chelation therapy (or phlebotomy if anemia is mild) should be started as early as possible to avoid iron overload, which can cause irreversible tissue damage. In addition, interferon-α is known to be effective for ameliorating anemia and iron accumulation in patients with CDA type 1, although the precise mechanism is still unknown (14). The survey data and our findings of the current case suggest that we should be aware of the possibility of CDA in patients with anemia and systemic iron overload at any age.

The authors state that they have no Conflict of Interest (COI).

References

1. Kamiya T, Manabe A. Congenital dyserythropoietic anemia. Int J Hematol **92**: 432-438, 2010.
2. Dgany O, Avidan N, Delaunay J, et al. Congenital dyserythropoietic anemia type I is caused by mutations in codanin-1. Am J Hum Genet **71**: 1467-1474, 2002.
3. Schwarz K, Iolascon A, Verissimo F, et al. Mutations affecting the secretory COPII coat component SEC23B cause congenital dyserythropoietic anemia type II. Nat Genet **41**: 936-940, 2009.
4. Heimpel H, Matuschek A, Ahmed M, et al. Frequency of congenital dyserythropoietic anemias in Europe. Eur J Haematol **85**: 20-25, 2010.
5. Kuribayashi T, Uchida S, Kuroume T, Umegae S, Omine M, Maekawa T. Congenital dyserythropoietic anemia type I: report of a pair of siblings in Japan. Blut **39**: 201-209, 1979.
6. Hiraoka A, Kanayama Y, Yonezawa T, Kitani T, Tarui S, Hashimoto PH. Congenital dyserythropoietic anemia type I: a freeze-fracture and thin section electron microscopic study. Blut **46**: 329-338, 1983.
7. Kato K, Sugitani M, Kawataki M, et al. Congenital dyserythropoietic anemia type 1 with fetal onset of severe anemia. J Pediatr Hematol Oncol **23**: 63-66, 2001.
8. Kanda J, Mizumoto C, Kawabata H, et al. Serum hepcidin level and erythropoietic activity after hematopoietic stem cell transplantation. Haematologica **93**: 1550-1554, 2008.
9. Pielage J, Stork T, Bunse I, Klämbt C. The Drosophila cell survival gene discs lost encodes a cytoplasmic Codanin-1-like protein, not a homolog of tight junction PDZ protein Patj. Dev Cell **5**: 841-851, 2003.
10. Renella R, Roberts NA, Brown JM, et al. Codanin-1 mutations in congenital dyserythropoietic anemia type 1 affect HP1α localization in erythroblasts. Blood **117**: 6928-6938, 2011.
11. Ganz T. Hepcidin and iron regulation, 10 years later. Blood **117**: 4425-4433, 2011.
12. Tamary H, Shalev H, Perez-Avraham G, et al. Elevated growth differentiation factor 15 expression in patients with congenital dyserythropoietic anemia type I. Blood **112**: 5241-5244, 2008.
13. Tanno T, Bhanu NV, Oneal PA, et al. High levels of GDF15 in thalassemia suppress expression of the iron regulatory protein hepcidin. Nat Med **13**: 1096-1101, 2007.
14. Lavabre-Bertrand T, Blanc P, Navarro R, et al. alpha-Interferon therapy for congenital dyserythropoiesis type I. Br J Haematol **89**: 929-932, 1995.

Treatment of acquired aplastic anemia in children

Seiji Kojima

Department of Pediatrics, Nagoya University Graduate School of Medicine, Nagoya, Japan

Aplastic anemia (AA) is an uncommon but serious disorder characterized by pancytopenia resulting from non-function of the bone marrow. The incidence of AA is approximately 3 fold more common in East Asia than in Europe and United States where yearly incidence rates are approximately two patients per one million.[1]

Keywords: Aplastic anemia, Children, Immunosuppressive therapy, Stem cell transplantation

Diagnosis of Childhood Aplastic Anemia

It is often difficult to distinguish hypoplastic myelodysplastic syndrome (MDS) from AA, especially in cases without cytogenetic abnormalities. Isolated anemia, which is the major presenting manifestation of refractory anemia (RA) in adults, is uncommon in children, who are more likely than adults to present with pancytopenia. In addition, hypocellularity of the bone marrow is more common in childhood RA. The new edition of the WHO classification for myeloid neoplasms outlines a provisional entity for refractory cytopenia for childhood (RCC) in which the diagnostic criteria for distinguishing RCC from AA are proposed.[2]

We studied the incidence and clinical feature of this new disease entity in Asian population with acquired bone marrow failure. A total of 100 children with cytopenia and hypocellular bone marrow (50 cases from Japan, 50 cases from China) were included in the present study. To obtain a diagnosis for cytopenia, at least two of the following must be present: (1) neutrophil count $<1.5 \times 10^9$/l; (2) hemoglobin <100 g/l; and (3) platelet count $<50 \times 10^9$/l. The severity of the disease was classified according to internationally accepted criteria.[3] AA patients exhibited no morphological changes in any of their hematopoietic cell lineages. RCC was defined as persistent cytopenia with <5% blasts in the bone marrow and <2% blasts in the peripheral blood. In addition, RCC patients had <10% dysplastic changes in >2 cell lineages, or >10% in 1 cell lineage. Patients classified as having refractory cytopenia with multilineage dysplasia (RCMD) exhibited >10% of the dysplastic changes in >2 cell lineages. Dysplastic features of bone marrow aspirate cytology and trephine biopsy sampled were evaluated according to recommendations by the French–American–British Cooperative Leukemia Working Group and the morphology group of the European Working Group of MDS in Childhood.[4,5] Final consensus for the diagnoses of 100 patients was follows: AA in 29 cases, RCC in 58 cases, and RCMD in 13 cases. The distribution of diagnoses were not different between Japanese cases and Chinese Cases; 12:17 in AA; 33:25 in RCC and 5:8 in RCMD, respectively. Among the three groups there were no significant differences with regard to median age at diagnosis, sex, or days from onset of symptoms to diagnosis. While eight out of 29 (28%) patients in the AA group had very severe cytopenia, only two of the 58 patients (3%) in the RCC group and none of the 13 patients in the RCMD group had very severe cytopenia. On the other hand, 45 of the 58 patients (78%) in the RCC group and 10 of the 13 patients (77%) of the RCMD group had non-severe cytopenia ($P<0.001$). Additionally, 16 out of 29 AA patients (55%) exhibited severe hypoplastic bone marrow cellularity, while only four out of 58 RCC patients (7%) and none of the RCMD patients had severe hypoplastic bone marrow. A number of the RCC/RCMD patients exhibited mild to moderate hypocellularity ($P<0.001$). Data for cytogenetic analyses were available from 75 patients. Abnormal karyotypes were detected in one patient from the AA group (47,XX,+8) and in three patients in the RCC group (47,XX,+8; 46,XY, t(x:3)(p11.2;q13); 49,idem,+6,+21).

The distribution of diagnoses in Japanese and Chinese children were 12:17 for AA; 33:25 for RCC and 5:8 for RCMD, respectively. Patients with RCC/RCMD were milder in disease severity and bone marrow hypocellularity, compared to those with AA. According to the WHO classification system, it is recommended that children who satisfy the criteria for RCMD should be considered as RCC until the numbers of lineages involved are fully evaluated whether it is an important prognostic discriminator in childhood MDS.[2] In the current study, 13 of the 71 MDS children (18%) were classified as RCMD. The bone marrow samples were more cellular, and dysplasia of cell morphology was more prominent in children with RCMD than those with RCC.

The most important aspect of the new proposal from the WHO classification system is whether the diagnosis has an impact on clinical outcomes including, response to treatment and incidence of late clonal diseases. Unfortunately, due to a short follow-up period and variety of treatments, we could not address this issue. To establish the new entity of RCC, future studies should prospectively compare the clinical outcomes between AA and RCC groups in a large number of patients.

First Line Treatment for Severe Aplastic Anemia in Children

Bone marrow transplantation (BMT) from an HLA-matched family donor (MFD) is the treatment of choice for severe aplastic anemia (SAA) in children. For children without an MFD, immunosuppressive therapy (IST) with a combination of antithymocyte globulin and cyclosporine has been successfully used.[6] However, this decision is based on the results of comparative studies of these two therapies mainly conducted in the 1980s, and the outcome of both BMT and IST has dramatically improved over the past three decades.[7,8] Therefore, updated evidences for treatment decision of pediatric SAA are required. We compared the outcome of children with SAA who received IST enrolled in the prospective multicenter trials of IST conducted by the Japan Childhood Aplastic Anemia Study Group[9,10] or BMT from an MFD registered to the Transplant Registry Unified Management Program conducted by the Japan Society for Hematopoietic Cell Transplantation. The influence of potential risk factors on overall survival (OS) and failure free survival (FFS) was assessed according to first line treatment, time periods of treatment (1992–1999 and 2000–2009), age and other variables related to each treatment. FFS was defined as survival with treatment response. Death, primary or secondary graft failure, relapse, and second malignancy were considered treatment failure in patients who received BMT. Death, relapse, disease progression requiring stem cell transplantation from an alternative donor or 2nd IST, clonal evolution, and evolution to paroxysmal nocturnal hemoglobinuria were considered treatment failure in patients who received IST. Between 1992 and 2009, 599 children with SAA younger than 17 years received BMT from an MFD (n=213) or IST (n=386) as a first line treatment. While the OS did not differ between patients received IST and BMT (88 ± 2 vs $90\pm2\%$ at 15 years), the FFS was significantly inferior in patients received IST than in those received BMT (54 ± 3 vs $84\pm3\%$ at 15 years, $P<0.0001$). There was no significant improvement of outcomes in the two time periods; OS and FFS at 10 years in 1992–1999 vs 2000–2009 were 87 ± 2 vs $93\pm2\%$ and 66 ± 3 vs $67\pm3\%$, respectively. In multivariate analysis, age <10 years was identified as a favorable factor for OS ($P=0.007$) and choice of the first line IST was the only risk factor for FFS ($P<0.0001$). These updated data support the current algorism for treatment decision which recommends BMT when an MFD is available.[6]

HLA-mismatched Family Donors BMT

The first-line therapy for children with severe AA is allogeneic BMT from a human leukocyte antigen (HLA)-matched family donor, and IST is indicated for patients without HLA-matched family donors.[6] While the standard therapy for children who fail to respond to IST is allogeneic BMT from an HLA-matched unrelated donor, BMT from an HLA-mismatched family donor has also been indicated. Compared with unrelated donors, an HLA-mismatched family donor has some advantages especially for children who need urgent transplantation.

We analyzed the clinical outcome of 578 children (325 boys and 253 girls) with AA (age, <20 years) who received allogeneic BMT between 1990 and 2009 in Japan, and registered to the Transplant Registry Unified Management Program. The median age at transplantation was 11 years (0–19), and the donors were serological 6/6 HLA-matched related donors (MRD) (n=312), one locus-mismatched related donor (1MMRD) (n=44), 2–3 loci-mismatched related (haploidentical) donors (n=9), and HLA-matched unrelated donors (MUD) (n=213). Causes of deaths were as follows: acute graft-versus-host disease (GVHD) (n=4), chronic GVHD (n=4), acute respiratory distress syndrome (n=2), severe hemorrhage (n=7), engraftment failure (n=5), infection (n=18), idiopathic pneumonia (n=8), organ failure (n=19), secondary malignancy (n=4), and others (n=4).

The probability of severe acute GVHD (grade III–IV) in patients transplanted from 1MMRD ($26.9\pm7.4\%$) was significantly higher than that in patients transplanted from MRD ($4.9\pm1.3\%$) ($P<0.001$). The probability of five-year overall survival (5y OS) of patients transplanted from 1MMRD ($93.1\pm3.9\%$)

Correspondence to: Seiji Kojima, Department of pediatrics, Nagoya University Graduate School of Medicine, 65, Tsurumai-cho, Showa-ku, Nagoya 466-8550, Japan. Email: kojimas@med.nagoya-u.ac.jp

DOI 10.1179/102453312X13336169155051